Major Oxide and Trace Element Geochemistry of Basement Rocks in the Ikole–Itapaji Area, Southwestern Nigeria: Implications for Metallic Mineralization Potential

***Adeleke Ojo, & Olusola Amos Olaolorun**

Department of Geology, Faculty of Physical Science, Ekiti State University, Ado Ekiti

***Corresponding Author**

DOI: https://doi.org/10.51244/IJRSI.2026.1307000069

Received: 12 July 2026; Accepted: 17 July 2026; Published: 28 July 2026

ABSTRACT

This study investigated the geology, petrogenesis, and mineralization potential of the crystalline rocks in the Ikole–Itapaji–Ake-Ako area, southwestern Nigeria, by integrating geological mapping with whole-rock major- and trace-element geochemistry. Detailed field mapping identified the dominant lithological units as migmatite, granite gneiss, granite, charnockite, and pegmatite, with well-developed structural features including foliations, joints, fractures, and quartz veins that provide favourable pathways for hydrothermal fluid circulation. Thirty-five fresh rock samples were collected during field investigations, from which twenty representative samples were selected for whole-rock geochemical analysis based on lithological representation, freshness, mineralogical diversity, textural and structural characteristics, and spatial distribution. Major-element analyses were carried out using Inductively Coupled Plasma–Mass Spectrometry (ICP–MS) following partial multi-acid digestion with hydrochloric acid (HCl), nitric acid (HNO_3), and perchloric acid ($HClO_4$), combined with lithium metaborate fusion to ensure complete dissolution of refractory silicate minerals and accurate determination of the major rock-forming elements. Major-oxide geochemistry was evaluated using Harker variation diagrams, the A/CNK–A/NK alumina saturation diagram, and the Fe-number discrimination diagram, while trace-element data were interpreted using factor analysis and correlation coefficient analysis. The Harker variation diagrams indicate that the studied rocks evolved predominantly through fractional crystallization, characterized by progressive depletion of MgO, FeOt, CaO, and TiO_2 with increasing SiO_2. The alumina saturation diagram shows that the rocks range from metaluminous to weakly peraluminous compositions, whereas the Fe-number discrimination diagram indicates predominantly magnesian affinities with minor transitional ferroan characteristics. Factor analysis identified Cu–Ni–Co–Fe–Zn as the principal mineralization association, explaining most of the geochemical variability, while As–Th–Ag–Pb constitute a secondary association related to lithological variation and hydrothermal alteration. Correlation coefficient analysis further revealed strong positive relationships among Cu, Ni, Co, Fe, and Zn, indicating a common geochemical source and structurally controlled magmatic–hydrothermal mineralization. The integrated geological and geochemical results demonstrate that the Ikole–Itapaji–Ake-Ako area possesses favourable conditions for sulphide mineralization and provide a valuable framework for future mineral exploration within the Precambrian Basement Complex of southwestern Nigeria.

Keywords: Ikole–Itapaji–Ake-Ako; Basement Complex; geological mapping; major-element geochemistry; trace-element geochemistry; fractional crystallization; factor analysis; mineralization.

INTRODUCTION

Precambrian crystalline basement rocks constitute the oldest preserved components of the continental crust and provide valuable records of crustal growth, magmatism, metamorphism, tectonic evolution, and mineralization through geological time. These rocks not only preserve evidence of the processes responsible for continental evolution but also host significant concentrations of metallic and industrial mineral resources, making them important targets for geological and mineral exploration studies. Consequently, whole-rock geochemistry has become one of the most reliable approaches for investigating the origin, evolution, and economic significance

ISSN No. 2321-2705 | DOI: 10.51244/IJRSI |Volume XIII Issue VII July 2026

of crystalline rocks because the chemical composition of rocks reflects their source characteristics, magmatic differentiation, tectonic environment, and post-magmatic modifications (Rollinson & Pease, 2021). Major oxide geochemistry provides information on magma composition and evolutionary trends, whereas trace elements serve as sensitive indicators of magma source, fractional crystallization, crustal contamination, hydrothermal alteration, and mineralization processes. The integration of these geochemical datasets therefore provides a robust framework for evaluating petrogenesis and assessing the metallic mineralization potential of crystalline basement terrains (Rollinson & Pease, 2021).

The Nigerian Basement Complex forms part of the Pan-African Mobile Belt that separates the West African and Congo cratons and consists predominantly of migmatite–gneiss complexes, schist belts, granitoids, charnockitic bodies, and pegmatitic intrusions emplaced during the Neoproterozoic Pan-African Orogeny. These lithological assemblages have experienced multiple episodes of deformation, metamorphism, magmatism, and crustal reworking, resulting in a complex geological framework that hosts numerous occurrences of gold, rare metals, pegmatite-related minerals, gemstones, and other economically important mineral deposits. The geological evolution and metallogenic significance of the Nigerian Basement Complex have been extensively documented, highlighting the influence of Pan-African tectonothermal events on crustal architecture and mineralization (Ajibade et al., 1987).

The Ikole–Itapaji area of southwestern Nigeria is underlain by diverse Precambrian lithological units comprising migmatite, granite gneiss, coarse porphyroblastic gneiss, granite, pegmatite, and charnockite. These rock units display varying mineralogical compositions and geochemical characteristics resulting from prolonged magmatic evolution, metamorphism, deformation, and weathering. Their compositional diversity suggests contrasting petrogenetic histories and varying capacities to host metallic mineralization. Consequently, detailed major oxide and trace element geochemical investigations are essential for understanding the evolution of these basement rocks and evaluating their mineral resource potential.

Previous investigations within the Nigerian Basement Complex have focused primarily on regional geology, tectonic evolution, petrography, structural relationships, and the metallogenic characteristics of different basement terranes (Rahaman, M. A. (1988)). Although these studies have significantly improved the understanding of the geological evolution of southwestern Nigeria, comprehensive whole-rock geochemical investigations that integrate major oxide and trace element data to evaluate the metallic mineralization potential of the Ikole–Itapaji basement rocks remain limited. In particular, the geochemical behaviour of economically important trace elements, elemental enrichment patterns, and their implications for mineral exploration within the study area have not been comprehensively evaluated. This knowledge gap limits a detailed understanding of the geochemical evolution of the basement rocks and constrains the identification of prospective lithological units for future mineral exploration.

This study therefore investigates the major oxide and trace element geochemistry of the basement rocks in the Ikole–Itapaji area, southwestern Nigeria, to evaluate their geochemical characteristics and implications for metallic mineralization potential. Specifically, the objectives of this study are to:

1. determine the major oxide and trace element compositions of the basement rocks in the Ikole–Itapaji area;
2. characterize the geochemical signatures of the different lithological units;
3. evaluate elemental enrichment and depletion patterns associated with metallic mineralization; and
4. assess the metallic mineralization potential of the study area using major oxide and trace element geochemistry.

The study area

Figure 1 presents the geographical location of the Ikole–Itapaji–Ake-Ako study area within Ekiti State, southwestern Nigeria. The inset map of Nigeria shows the position of Ekiti State within the southwestern region of the country, while the highlighted rectangle delineates the precise location of the study area. The area lies within the Precambrian Basement Complex of southwestern Nigeria**,** which forms part of the Pan-African mobile belt situated between the West African and Congo Cratons. The Nigerian Basement Complex is characterized by widespread migmatite–gneiss complexes, Pan-African granitoids, charnockitic bodies,

ISSN No. 2321-2705 | DOI: 10.51244/IJRSI |Volume XIII Issue VII July 2026

pegmatites, and minor metasedimentary rocks that have undergone multiple episodes of deformation, metamorphism, and magmatism (Rahaman, 1988).

The enlarged topographic map shows that the study area extends approximately between latitudes 7°47′N and 8°05′N and longitudes 5°26′E and 5°34′E, covering an estimated surface area of about 590 km². The contour pattern indicates a rugged and undulating terrain characterized by numerous hills, ridges, and valleys, which are typical geomorphological features of crystalline basement terrains. Closely spaced contour lines represent steep slopes and elevated ridges, whereas widely spaced contours indicate relatively gentle slopes and low-lying areas. Such topographic variations are largely controlled by differences in lithology, weathering resistance, and structural deformation within the basement rocks (Ojo et al., 2024).

The drainage pattern displayed on the map is predominantly dendritic, indicating that stream development is mainly controlled by the regional slope and the relatively homogeneous crystalline bedrock. However, local variations in stream orientation may reflect the influence of fractures, joints, and faults that commonly characterize the Nigerian Basement Complex. Structural discontinuities frequently serve as zones of weakness that guide surface drainage and facilitate groundwater movement and hydrothermal fluid circulation (Adetunla et al., 2025).

The road network shown on the map indicates that the study area is relatively accessible through major and minor roads linking Ikole-Ekiti, Itapaji, and Ake-Ako. This accessibility facilitated detailed geological mapping, structural measurements, and representative rock-sample collection during the field investigation. The combination of extensive rock exposures, rugged topography, and well-developed drainage provides favourable conditions for geological mapping and mineral exploration within the area (Ajibade & Rahaman 1987).

Overall, the location and physiographic characteristics illustrated in Figure 1 indicate that the Ikole–Itapaji–Ake-Ako area possesses the geological and structural attributes typical of the southwestern Nigerian Basement Complex. The presence of resistant crystalline rocks, pronounced topographic relief, and structurally controlled drainage provides a favourable geological framework for investigating the petrogenesis, geochemical evolution, and mineralization potential of the basement rocks.

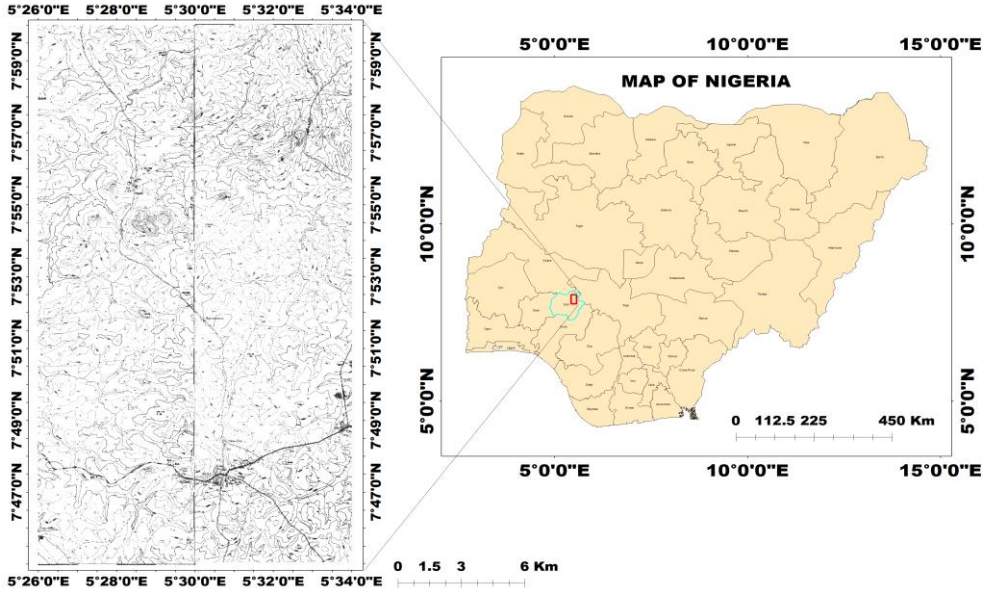

Figure 1. Location and topographic map of the Ikole–Itapaji–Ake-Ako area, Ekiti State, southwestern Nigeria, illustrating the geographical extent, drainage network, road accessibility, and topographic relief of the study area.

Geological setting

The study area is located within southwestern Nigeria, forming part of the Precambrian Basement Complex of the West African Craton. This crystalline basement terrain is distinct from the surrounding sedimentary basins,

ISSN No. 2321-2705 | DOI: 10.51244/IJRSI |Volume XIII Issue VII July 2026

including the Sokoto Basin, Chad Basin, Bida Basin, and the Benue Trough, which are largely composed of Cretaceous-to-Tertiary sediments (Ojo et al., 2024). The southwestern region, including the Ikole–Itapaji axis, is dominated by crystalline rocks that have undergone extensive tectono-metamorphic evolution. The Nigerian Basement Complex evolved through multiple orogenic events, notably the Liberian, Eburnean, and Pan-African cycles, which resulted in widespread deformation, metamorphism, and granitoid emplacement (Adetunla et al., 2025). These processes led to the development of major lithological units, including the migmatite–gneiss complex, schist belts, and Pan-African granitoids.

In the study area, migmatite–gneiss and granitic rocks are predominant, with minor metasedimentary occurrences. Structurally, the area is characterized by well-developed faults, fractures, and foliations, predominantly trending NE–SW and NW–SE, reflecting the imprint of Pan-African deformation (Ogah & Abubakar, 2024). These structures are critical in controlling hydrothermal fluid flow and mineral deposition. Mineralization within the Basement Complex is commonly associated with quartz veins, pegmatites, and shear zones. The presence of granitic and pegmatitic intrusions within the Ikole–Itapaji area further suggests favourable conditions for mineralization. Recent studies have demonstrated the effectiveness of integrated geophysical methods in delineating such structurally controlled mineralized zones (Salako et al., 2024). The geological framework of the study area reflects a complex interplay of lithology and structure, providing a suitable environment for mineralization and justifying integrated geophysical and remote sensing investigations (Fig. 2)

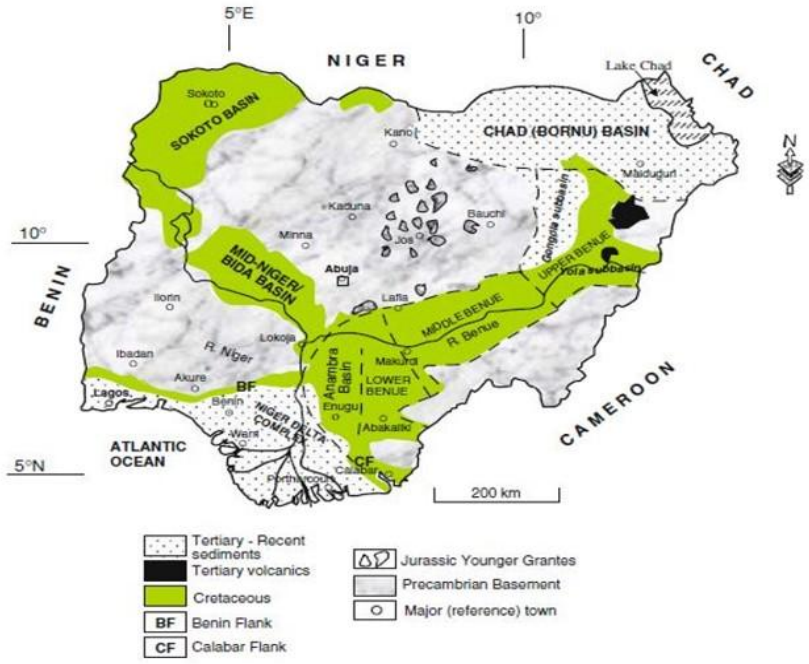

Figure 2: Geological map of Nigeria showing the distribution of major lithological units, including the Precambrian Basement Complex and surrounding sedimentary basins (Sokoto, Chad, Bida, and Benue Trough). The study area (Ikole–Itapaji, southwestern Nigeria) is located within the Basement Complex.

Topographic Map Showing Geological Sampling Locations

The topographic map Figure 3 illustrates the spatial distribution of geological sampling locations across the Ikole–Itapaji–Bolorunduro–Odo Oro–Ake-Ako area. The sampling points are well distributed throughout the study area, extending from the southern part around Ikole and Odo Oro through Bolorunduro to the northern sectors around Itapaji and Ake-Ako. This broad spatial coverage ensures that all the major lithological units identified within the study area are adequately represented and provides a reliable basis for subsequent geological, structural, petrographic, and geochemical investigations (Ogah & Abubakar, 2024).

The density of sampling points is noticeably higher around the Itapaji, Ake-Ako, and northern portions of the study area, where rugged topography and relatively high elevations provide abundant fresh basement rock exposures. These elevated terrains expose crystalline rocks with minimal weathering, thereby facilitating direct

ISSN No. 2321-2705 | DOI: 10.51244/IJRSI |Volume XIII Issue VII July 2026

observation of lithological contacts, structural features, and representative rock sampling. Conversely, relatively fewer sampling locations occur around Odo Oro and the southern part of Ikole, where the terrain is comparatively gentle and extensive soil development, vegetation cover, and weathered overburden locally obscure the basement rocks, thereby reducing outcrop availability (Ojo et al., 2024).

The sampling locations are distributed across ridges, hillslopes, valleys, and gently undulating terrains, thereby minimizing spatial bias and ensuring that lithological variations are examined under different geomorphological settings. This distribution also enhances the recognition of structural elements such as foliations, joints, fractures, quartz veins, folds, and lineaments that are commonly better exposed on elevated and dissected terrains. The widespread distribution of sampling points therefore improves the reliability of structural interpretations and provides adequate coverage for correlating lithological variations with topographic expression across the study area (Salako et al., 2024).

Furthermore, the sampling strategy captures the spatial occurrence of the major crystalline rock units, including migmatite, granite gneiss, coarse porphyroblastic gneiss, granite, pegmatite, and charnockite, thereby ensuring that the petrographic and geochemical datasets are representative of the geological diversity of the Ikole–Itapaji–Ake-Ako Basement Complex. The comprehensive distribution of the sampling points also provides a sound framework for evaluating mineralogical variations, petrogenesis, tectonic evolution, and mineralization potential across the study area (Adetunla et al., 2025).

Overall, the spatial distribution of the sampling locations demonstrates a systematic and representative sampling strategy that adequately covers the entire study area. The combination of extensive geographical coverage, representation of all major lithological units, and sampling across different topographic settings provides a robust foundation for geological mapping, structural analysis, petrographic characterization, geochemical evaluation, and interpretation of the tectonometamorphic evolution of the Ikole–Itapaji–Bolorunduro–Odo Oro–Ake-Ako area within the Precambrian Basement Complex of southwestern Nigeria (Oyinloye 2011).

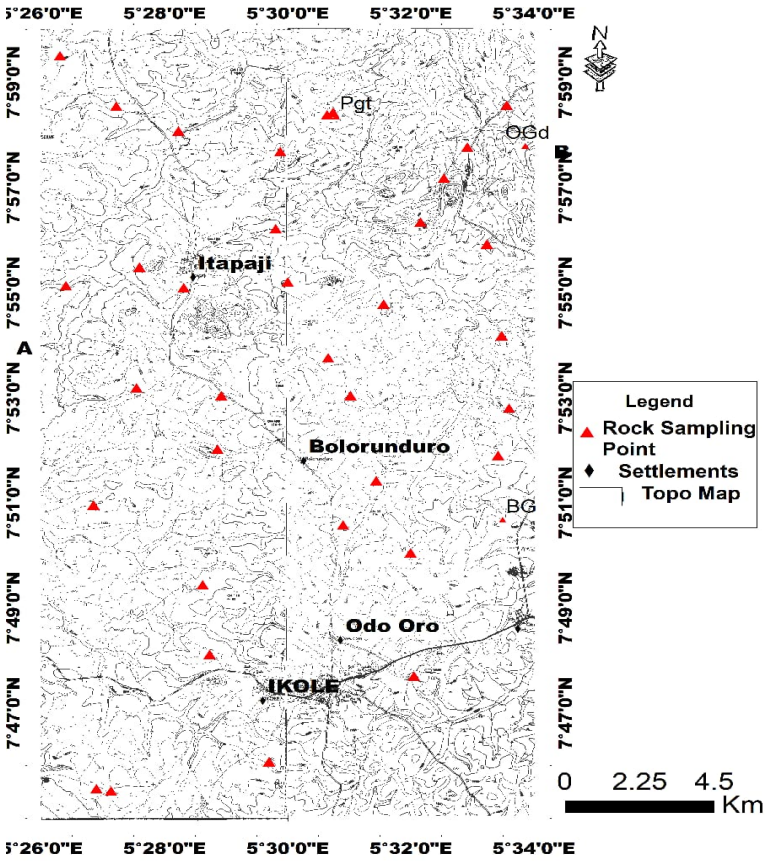

Figure 3. Topographic map of the Ikole–Itapaji–Ake-Ako area, Southwestern Nigeria, showing the distribution of geological sampling points used for geological mapping, structural measurements, and petrographic investigations. The sampling locations provide representative coverage of the major basement rock units across the study area.

ISSN No. 2321-2705 | DOI: 10.51244/IJRSI |Volume XIII Issue VII July 2026

The geological map and accompanying cross-section, Figure 4 reveals that the Ikole–Itapaji–Ake-Ako area is underlain predominantly by rocks of the Precambrian Basement Complex comprising migmatite (Mg), granite gneiss (GG), charnockite (Ch), granodiorite (OGd), and minor pegmatite intrusions. The spatial distribution of these lithologies indicates a complex geological history involving high-grade metamorphism, partial melting, magmatic emplacement, and crustal reworking during the Pan-African tectonothermal event.

The geological map shows that granite gneiss constitutes the dominant lithological unit**,** occupying a large proportion of the central and northern parts of the study area. This unit extends continuously from Itapaji through Bolorunduro and towards the northeastern portion of the map, suggesting that granite gneiss forms the principal basement framework of the area. Field and petrographic evidence indicate that the granite gneiss is characterized by quartz, feldspar, biotite, and muscovite assemblages typical of amphibolite- to granulite-facies metamorphism.

Migmatite occurs extensively in the southern portion of the study area around Ikole and Odo Oro. The broad distribution of migmatite suggests widespread partial melting and anatexis within the basement rocks. The gradational contact observed between migmatite and granite gneiss indicates that both lithologies share a common tectonometamorphic history, with migmatite representing zones of more intense partial melting and metamorphic reworking (Rahaman, 1988; Oyinloye, 2011).

The charnockite body exposed in the southwestern portion of the map occurs as a relatively restricted lithological unit. Its limited areal extent suggests emplacement or preservation as an isolated body within the surrounding granite gneiss terrain. Charnockitic rocks are generally associated with deep crustal processes and high-temperature metamorphism, indicating that parts of the study area experienced elevated thermal conditions during crustal evolution (Adetunla et al., 2025).

The granodiorite body located in the northeastern section of the map forms a discrete intrusive mass. The cross-section demonstrates that the granodiorite extends to depth and is not merely a superficial exposure. This geometry suggests emplacement as a plutonic body intruding the surrounding granite gneiss. The presence of pegmatite veins associated with the granodiorite further supports late-stage magmatic differentiation and residual melt emplacement during the final stages of crystallization (Ayuba et al., 2024).

The geological cross-section along A–B Figure 4 illustrates the subsurface relationships between the major lithological units. Granite gneiss occupies most of the intermediate crustal section and overlies a broad migmatitic basement. The undulating contact between granite gneiss and migmatite suggests an irregular basement surface produced by differential melting, metamorphic segregation, and prolonged crustal evolution. The continuity of the migmatite beneath much of the section indicates that it forms the oldest exposed basement unit within the area.

The cross-section further demonstrates that the granodiorite intrusion cuts the surrounding granite gneiss in the northeastern segment of the profile. This intrusive relationship indicates that the granodiorite is younger than the host granite gneiss. The pegmatite body shown within the granodiorite represents a later magmatic phase formed by crystallization of residual silica-rich melts. Such pegmatitic intrusions are common products of highly evolved granitic systems and frequently host economically important rare-element minerals (Adetunla et al., 2025).

From a geological evolution perspective, the study area records multiple stages of crustal development. The migmatites represent the oldest basement components formed through high-grade metamorphism and partial melting. These were subsequently reworked and transformed into granite gneiss during regional metamorphic events. Charnockitic bodies were emplaced or developed under high-temperature conditions, while granodioritic magmatism and pegmatitic intrusions represent younger intrusive phases associated with crustal melting and magmatic differentiation. Collectively, these lithological relationships indicate prolonged Precambrian crustal evolution culminating in widespread Pan-African tectono-metamorphism (Rahaman, 1988; Oyinloye, 2011).

ISSN No. 2321-2705 | DOI: 10.51244/IJRSI |Volume XIII Issue VII July 2026

The geological architecture depicted by the map and cross-section demonstrates that the Ikole–Itapaji–Ake-Ako area forms part of a deeply reworked basement terrane characterized by extensive migmatization, granitoid emplacement, and localized charnockitic development. The intimate association of these lithologies provides evidence of repeated episodes of metamorphism, partial melting, magmatism, and crustal stabilization within the southwestern Nigerian Basement Complex.

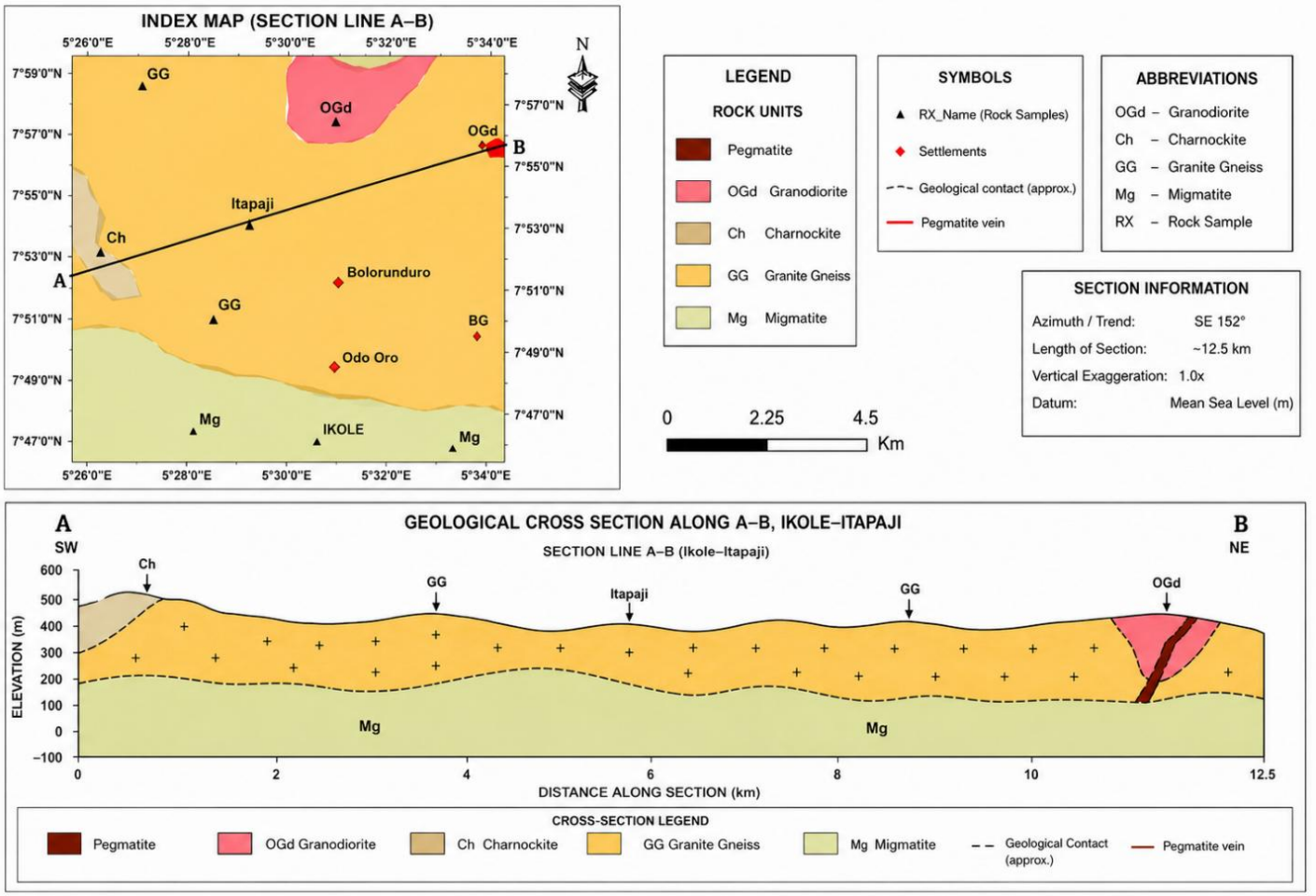

Figure 4. Geological cross-section along A–B across the Ikole-Itapaji area, showing the subsurface relationships between migmatite, granite gneiss, charnockite, granodiorite, and pegmatite units. The section reveals a migmatitic basement overlain by granite gneiss and intruded by younger granodiorite and pegmatite bodies. The geometry of the rock units reflects prolonged crustal evolution involving metamorphism, partial melting, and magmatic emplacement within the Precambrian Basement Complex.

MATERIALS AND METHODS

Materials

The materials used for this study comprised field and laboratory equipment required for geological mapping, structural measurements, rock sample collection, and whole-rock geochemical analyses. Field equipment included a 1:25,000-scale topographic map of the Ikole–Itapaji–Ake-Ako area, a Brunton compass clinometer, a Garmin GPSMAP 64s handheld Global Positioning System (GPS), a geological hammer, chisel, hand lens, measuring tape, sample bags, permanent markers, a field notebook, digital camera, and personal protective equipment comprising safety boots, reflective jacket, hand gloves, and a safety helmet. These materials facilitated geological mapping, structural measurements, accurate location referencing, documentation of field observations, and the collection of representative fresh rock samples.

Laboratory equipment consisted of a diamond rock-cutting machine, jaw crusher, pulverizing machine, analytical weighing balance, and computer software for geochemical data processing, statistical analyses, and

ISSN No. 2321-2705 | DOI: 10.51244/IJRSI |Volume XIII Issue VII July 2026

graphical presentation of results. Whole-rock geochemical analyses were conducted at ACME Analytical Laboratories (Bureau Veritas Commodities Canada Ltd.), Vancouver, Canada, using internationally accepted analytical procedures for the determination of major oxides and trace elements.

Methods

The study commenced with a reconnaissance survey of the Ikole–Itapaji–Ake-Ako area using a 1:25,000-scale topographic map to obtain preliminary information on accessibility, drainage pattern, topography, and distribution of rock exposures. The reconnaissance exercise provided the basis for planning geological traverses and ensuring adequate spatial coverage during detailed field investigations.

Detailed geological mapping was subsequently carried out along accessible roads, footpaths, stream channels, farm tracks, and exposed rock outcrops. Lithological characteristics including colour, grain size, texture, mineral composition, weathering characteristics, and field relationships were carefully observed and documented. Structural features such as foliations, joints, fractures, folds, mineral lineations, quartz veins, and shear zones were identified, while their strike and dip were measured using a Brunton compass clinometer. The geographical coordinates and elevations of each outcrop were recorded using a Garmin GPSMAP 64s handheld GPS receiver, and representative field photographs were taken to document important geological features. The field observations were subsequently used in the preparation of the geological map and geological cross-sections of the study area.

A total of thirty-five (35) fresh rock samples representing the major lithological units encountered during geological mapping, including migmatite, granite gneiss, coarse porphyroblastic gneiss, granite, pegmatite, and charnockite, were collected from different locations across the study area. Following detailed megascopic examination, twenty (20) representative samples were selected for whole-rock geochemical analyses based on the following criteria:

1. Representation of all the major lithological units identified during geological mapping.

2. Freshness of the rock samples, with preference given to fresh, unweathered, and minimally altered specimens.

3. Lithological and mineralogical diversity to ensure adequate representation of the compositional variability of the different rock units within the study area.

4. Megascopic textural variability, including differences in grain size, mineral fabric, and weathering characteristics observed during field examination.

5. Structural characteristics, particularly samples exhibiting representative foliations, mineral banding, folds, quartz veins, and shear fabrics.

6. Spatial distribution to ensure adequate geographical representation of the different lithological units across the study area.

7. Elimination of duplicate samples exhibiting similar lithological, mineralogical, and structural characteristics from the same locality to avoid analytical redundancy while maintaining representative coverage.

This selection procedure ensured that the analysed samples adequately represented the lithological, structural, and compositional variability of the crystalline basement rocks within the study area.

Fresh portions of the selected rock samples were cleaned to remove weathered surfaces before being reduced to smaller fragments using a jaw crusher and subsequently pulverized into fine homogeneous powders. The pulverized samples were packaged and submitted to ACME Analytical Laboratories (Bureau Veritas Commodities Canada Ltd.), Vancouver, Canada, for whole-rock geochemical analyses.

ISSN No. 2321-2705 | DOI: 10.51244/IJRSI |Volume XIII Issue VII July 2026

The selected twenty (20) representative samples for whole-rock geochemical analyses were cleaned to remove weathered surfaces before being crushed using a jaw crusher and pulverized into fine homogeneous powders. The pulverized samples were packaged and transported to ACME Analytical Laboratories (Bureau Veritas Commodities Canada Ltd.), Vancouver, Canada, for chemical analysis. Major-element analyses were carried out using Inductively Coupled Plasma–Mass Spectrometry (ICP–MS) following partial multi-acid digestion with hydrochloric acid (HCl), nitric acid (HNO_3), and perchloric acid ($HClO_4$), combined with lithium metaborate fusion. The lithium metaborate fusion technique ensured complete dissolution of refractory silicate minerals, while the acid digestion enhanced the extraction and determination of the major rock-forming elements. Quality assurance and quality control (QA/QC) procedures included the analysis of certified reference materials, analytical blanks, duplicate samples, and internal laboratory standards to ensure the accuracy, precision, and reliability of the analytical results.

Geochemical Data Analysis

The whole-rock geochemical data were processed to evaluate the geochemical characteristics, magmatic evolution, and metallic mineralization potential of the basement rocks within the Ikole–Itapaji–Ake-Ako area. Major oxide data were interpreted using Harker variation diagrams to evaluate compositional variations and magmatic differentiation trends among the different lithological units. The degree of alumina saturation was assessed using the A/CNK–A/NK alumina saturation diagram after Shand (1943), while the magmatic affinity of the rocks was further evaluated using the Fe-number [FeOt/ (FeOt + MgO)] versus SiO_2 discrimination diagram proposed by Frost et al. (2001).

Trace element data were statistically evaluated using Pearson correlation coefficient analysis to determine elemental relationships and identify possible geochemical associations among the analysed elements. Factor analysis was further employed to identify the principal geochemical processes controlling elemental distribution and to delineate elemental associations related to lithological variation and metallic mineralization potential within the study area. The integration of geological field observations with major oxide and trace element geochemistry provided a comprehensive framework for interpreting the geochemical evolution and metallic mineralization potential of the crystalline basement rocks in the Ikole–Itapaji–Ake-Ako area.

RESULTS AND DISCUSSION

Major oxides geochemistry (Charnockite)

The Harker variation diagrams Figure 5 illustrate the relationship between SiO_2 and the major oxides (Al_2O_3, MgO, CaO, Na_2O, K_2O, TiO_2, P_2O_5, and FeOt) for the charnockitic rocks from the Ikole–Itapaji–Ake-Ako area. Despite the limited number of samples, the diagrams reveal systematic geochemical trends that provide insight into the magmatic evolution of the rocks.

The concentrations of MgO, CaO, TiO_2, and FeOt decrease with increasing SiO_2**,** indicating that the magma became progressively depleted in ferromagnesian components during differentiation. This trend is characteristic of fractional crystallization involving the early removal of mafic minerals such as pyroxene, amphibole, biotite, Fe–Ti oxides, and calcic plagioclase from the evolving magma (Irzon, R., (2013). The decrease in CaO further suggests continuous plagioclase fractionation, while the reduction in TiO_2 and FeOt reflects the crystallization of Fe–Ti oxide minerals.

Conversely, K_2O, Na_2O, Al_2O_3, and P_2O_5 exhibit positive correlations with increasing SiO_2**.** The enrichment of K_2O and Na_2O indicates progressive concentration of alkali feldspars during the late stages of magma evolution, whereas the slight increase in Al_2O_3 reflects the abundance of feldspar phases within the felsic fraction. The increase in P_2O_5 may be attributed to the delayed crystallization of apatite, allowing phosphorus to accumulate in the residual melt before saturation (Hayatu, R. A. (2024).

The observed geochemical trends are consistent with the differentiation of a common parental magma through fractional crystallization, resulting in the production of more evolved, silica-rich charnockitic compositions. Similar Harker variation patterns have been reported for granitoid and charnockitic suites worldwide, where

ISSN No. 2321-2705 | DOI: 10.51244/IJRSI |Volume XIII Issue VII July 2026

systematic depletion of compatible elements and enrichment of incompatible elements reflect progressive magmatic differentiation (Oyebamiji et al., 2024).

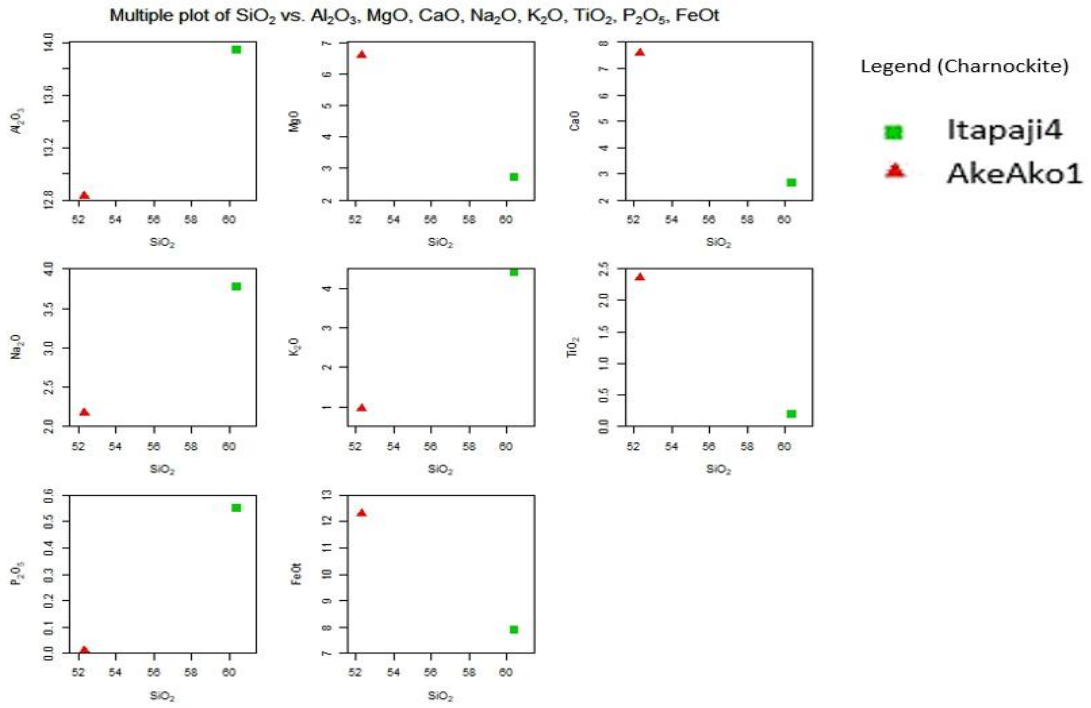

Figure 5. Harker variation diagrams showing the relationships between SiO_2 and the major oxides (Al_2O_3, MgO, CaO, Na_2O, K_2O, TiO_2, P_2O_5, and FeOt) for the charnockitic rocks from the Ikole–Itapaji–Ake-Ako area. The diagrams indicate systematic geochemical variations consistent with fractional crystallization and progressive magmatic differentiation (after Peccerillo & Taylor, 1976).

The A/CNK–A/NK diagram Figure 6, proposed by Shand (1943), is widely used to classify granitoids according to their alumina saturation characteristics. The diagram distinguishes peralkaline, metaluminous, and peraluminous rocks based on the molecular proportions of Al_2O_3, CaO, Na_2O, and K_2O. The two analyzed charnockitic samples from the Ikole–Itapaji–Ake-Ako area plot within the metaluminous field, indicating that the rocks contain sufficient Ca, Na, and K relative to Al to accommodate aluminium within feldspars and ferromagnesian silicates without the formation of peraluminous minerals.

The Itapaji4 sample plots close to the boundary separating the metaluminous and peralkaline fields (A/CNK ≈ 0.88), whereas the AkeAko1 sample occupies a more central position within the metaluminous field (A/CNK ≈ 0.70). Despite this variation, both samples exhibit A/CNK values less than 1.0, confirming their metaluminous character. Metaluminous granitoids are typically dominated by hornblende, biotite, pyroxene, and plagioclase and are generally interpreted to have crystallized from mantle-derived or lower crustal magmas with limited crustal contamination (Oyebamiji et al., 2024).

The absence of peraluminous compositions suggests that the parental magma did not undergo significant aluminium enrichment through crustal anatexis or extensive assimilation of pelitic sedimentary material. Instead, the metaluminous nature of the studied charnockites is consistent with magmatic differentiation dominated by fractional crystallization of mafic silicates and feldspars. Recent geochemical investigations have shown that metaluminous granitoids commonly originate from I-type magmatic systems generated in subduction-related or post-collisional tectonic environments, where mantle-derived magmas evolve through crystallization with only minor crustal interaction (Irzon, R., (2013).

The relatively higher A/NK value of the AkeAko1 sample reflects a greater proportion of alumina relative to alkalis compared to the Itapaji4 sample; however, both samples remain firmly within the metaluminous domain. This compositional similarity indicates that the analyzed charnockites are genetically related and

ISSN No. 2321-2705 | DOI: 10.51244/IJRSI |Volume XIII Issue VII July 2026

likely evolved from a common parental magma through progressive fractional crystallization rather than through fundamentally different petrogenetic processes.

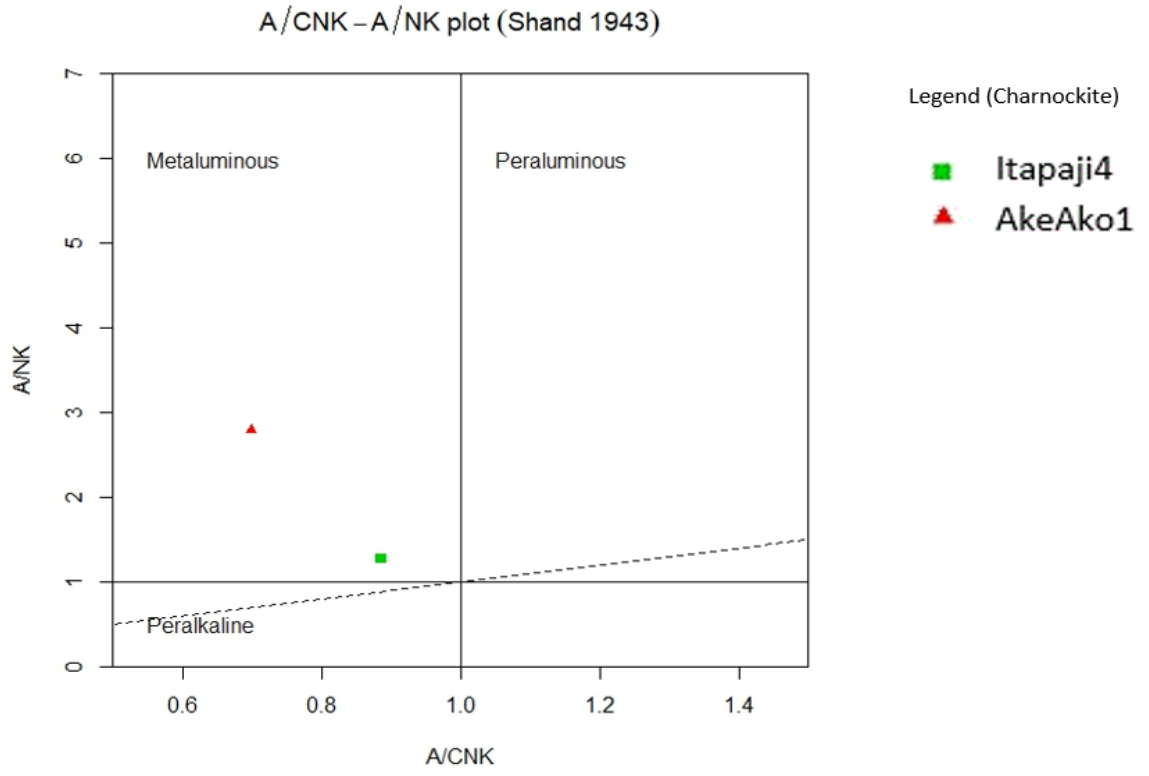

Figure 6. A/CNK–A/NK alumina saturation diagram after Shand (1943) showing that the analyzed charnockitic samples from the Ikole–Itapaji–Ake-Ako area plot within the metaluminous field, indicating crystallization from mantle-influenced magmas with limited crustal contamination.

The Fe-number versus SiO_2 diagram Figure 7, proposed by Frost et al. (2001)**,** classifies granitoid rocks into ferroan and magnesian series based on the ratio FeOt/ (FeOt + MgO)**.** This classification provides important insights into magma evolution, oxidation state, and tectonic setting. The analyzed charnockitic samples from the Ikole–Itapaji–Ake-Ako area plot on opposite sides of the discrimination boundary, indicating slight variations in their magmatic evolution (Clemens, (2003).

The Itapaji4 sample plots within the ferroan field, indicating enrichment in total iron relative to magnesium. Ferroan granitoids are generally associated with iron-enriched magmas that evolve under relatively reduced conditions through extensive fractional crystallization. Such magmas are commonly linked to anorogenic, extensional, or post-collisional tectonic environments, where prolonged magmatic differentiation promotes iron enrichment in the residual melt (Oyebamiji et al., 2024).

In contrast, the AkeAko1 sample plots within the magnesian field, suggesting a comparatively higher magnesium content relative to total iron. Magnesian granitoids are typically interpreted as products of relatively oxidized magmatic systems in which early crystallization of Fe–Ti oxide minerals limits iron enrichment while preserving relatively higher Mg contents. This compositional characteristic is commonly associated with calc-alkaline magmatic suites generated in convergent or continental arc environments (Irzon, R., (2013).

The proximity of both samples to the ferroan–magnesian discrimination boundary indicates that the charnockitic suite exhibits transitional geochemical characteristics rather than representing two fundamentally distinct magma types. The observed variation may reflect differences in the degree of fractional crystallization, oxidation state, or local compositional heterogeneity within a genetically related magma. Such transitional

ISSN No. 2321-2705 | DOI: 10.51244/IJRSI |Volume XIII Issue VII July 2026

behaviour has been documented in differentiated granitoid complexes where minor variations in Fe/Mg ratios occur during magma evolution (Oyebamiji et al., 2024).

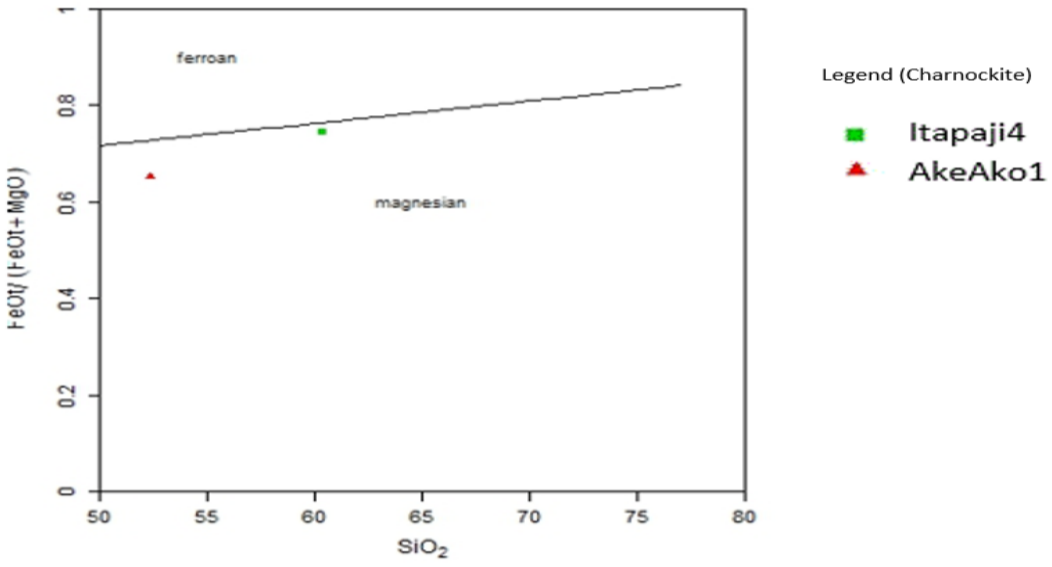

Figure 7. Fe-number (FeOt/ (FeOt + MgO)) versus SiO_2 discrimination diagram after Frost et al. (2001) showing that the charnockitic samples from the Ikole–Itapaji–Ake-Ako area exhibit both ferroan and magnesian affinities, indicating variations in iron enrichment during magmatic differentiation.

Major oxides geochemistry (granite)

The Harker variation diagrams Figure 8 illustrate the relationships between SiO_2 and the major oxides (Al_2O_3, MgO, CaO, Na_2O, K_2O, TiO_2, P_2O_5, and FeOt) for the granite samples collected from the Igbona–Ikole area within the Ikole–Itapaji–Ake-Ako Basement Complex. The diagrams were used to evaluate the geochemical evolution of the granites and identify the magmatic processes responsible for their compositional variation. Although only two representative samples (Igbona–Ikole 1 and Igbona–Ikole 2) were analyzed, the geochemical trends provide valuable evidence of magma differentiation.

The Igbona–Ikole 2 sample, which possesses the higher SiO_2 content (approximately 72 wt.%), exhibits lower concentrations of Al_2O_3 and FeOt than the Igbona–Ikole 1 sample. These decreases indicate progressive depletion of iron-bearing minerals and aluminosilicate phases during fractional crystallization. The reduction in FeOt reflects early crystallization of ferromagnesian minerals and Fe–Ti oxides, while the slight decrease in Al_2O_3 suggests continued fractionation of feldspars during magma evolution (Oyebamiji et al., 2024).

In contrast, the Igbona–Ikole 2 sample shows slightly higher concentrations of MgO, CaO, K_2O, TiO_2, and P_2O_5 than the Igbona–Ikole 1 sample. Although these positive relationships are not typical of large granitoid datasets, they most likely reflect the very limited number of analyzed samples rather than true geochemical trends. The increase in K_2O indicates enrichment of potassium during differentiation and suggests abundant K-feldspar crystallization in the later stages of magma evolution. Likewise, the relatively high Na_2O contents indicate the continued importance of alkali feldspars within the felsic magma (Barbarin, B. (1999).

Both Igbona–Ikole 1 and Igbona–Ikole 2 possess high silica contents (68–72 wt.% SiO_2), confirming that they are highly evolved felsic granites. Their limited compositional variation suggests derivation from a common calc-alkaline parental magma that had already undergone substantial differentiation prior to emplacement. Such geochemical characteristics are typical of continental granitoids formed through prolonged fractional crystallization (Oyebamiji et al., 2024).

ISSN No. 2321-2705 | DOI: 10.51244/IJRSI |Volume XIII Issue VII July 2026

The Harker variation patterns agree with the AFM diagram, which classifies the granites within the calc-alkaline series, the TAS diagrams that place the samples within the dacite and rhyolite fields, the A/CNK–A/NK diagram indicating metaluminous to weakly peraluminous compositions, and the Fe-number diagram showing a magnesian affinity. Collectively, these geochemical characteristics indicate that the Igbona–Ikole granites evolved through progressive fractional crystallization of a calc-alkaline parental magma with only minor chemical variation.

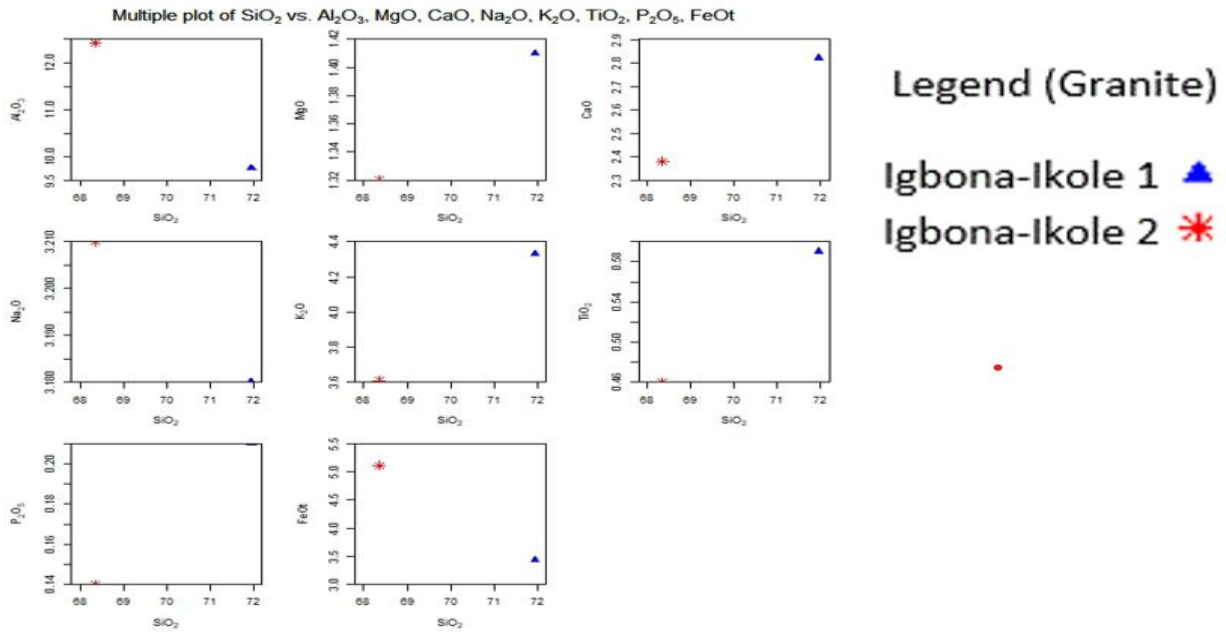

Figure 8. Harker variation diagrams showing the relationships between SiO_2 and the major oxides (Al_2O_3, MgO, CaO, Na_2O, K_2O, TiO_2, P_2O_5, and FeOt) for the granitic rocks from the Ikole–Itapaji–Ake-Ako area. The observed geochemical variations suggest progressive fractional crystallization and magmatic differentiation (after Peccerillo & Taylor, 1976).

The A/CNK–A/NK diagram Figure 9, after Shand (1943)**,** classifies the granitic rocks of the Ikole–Itapaji–Ake-Ako area according to their alumina saturation characteristics. The diagram distinguishes peralkaline**,** metaluminous**,** and peraluminous granitoids using the molecular proportions of Al_2O_3, CaO, Na_2O, and K_2O. The two granite samples (Igbona-Ikole1 and Igbona-Ikole 2**)** exhibit contrasting alumina saturation characteristics, indicating compositional variability within the granitic suite.

The Igbona-Ikole 2 sample plots within the metaluminous field, with an A/CNK value less than 1.0, indicating that aluminium is balanced by calcium, sodium, and potassium and is accommodated primarily within feldspars and ferromagnesian minerals. Metaluminous granites are commonly classified as I-type granitoids and are generally derived from mantle-influenced or lower crustal magmas that evolve through fractional crystallization with limited crustal contamination (Barbarin, B. (1999).

In contrast, the Igbona-Ikole1 sample plots within the peraluminous field, with an A/CNK value approaching unity. This indicates a slight excess of aluminium relative to Ca, Na, and K, suggesting the possibility of minor crustal assimilation or partial melting of aluminium-rich crustal materials during magma evolution. Peraluminous granites are commonly associated with more evolved magmatic systems and may contain aluminium-rich minerals such as muscovite, garnet, or cordierite where the degree of peraluminosity is sufficiently high (Clemens, (2003).

The occurrence of both metaluminous and weakly peraluminous compositions suggests that the granitic suite underwent variable degrees of magmatic differentiation and crustal interaction. However, the close proximity of the two samples on the diagram indicates that these differences are relatively minor and likely represent

ISSN No. 2321-2705 | DOI: 10.51244/IJRSI |Volume XIII Issue VII July 2026

progressive evolution of a genetically related magma rather than derivation from entirely separate magma sources. Similar transitions from metaluminous to weakly peraluminous compositions have been reported in differentiated granitic plutons, where prolonged fractional crystallization and limited crustal contamination modify the alumina saturation index during magma evolution (Irzon, R., (2013).

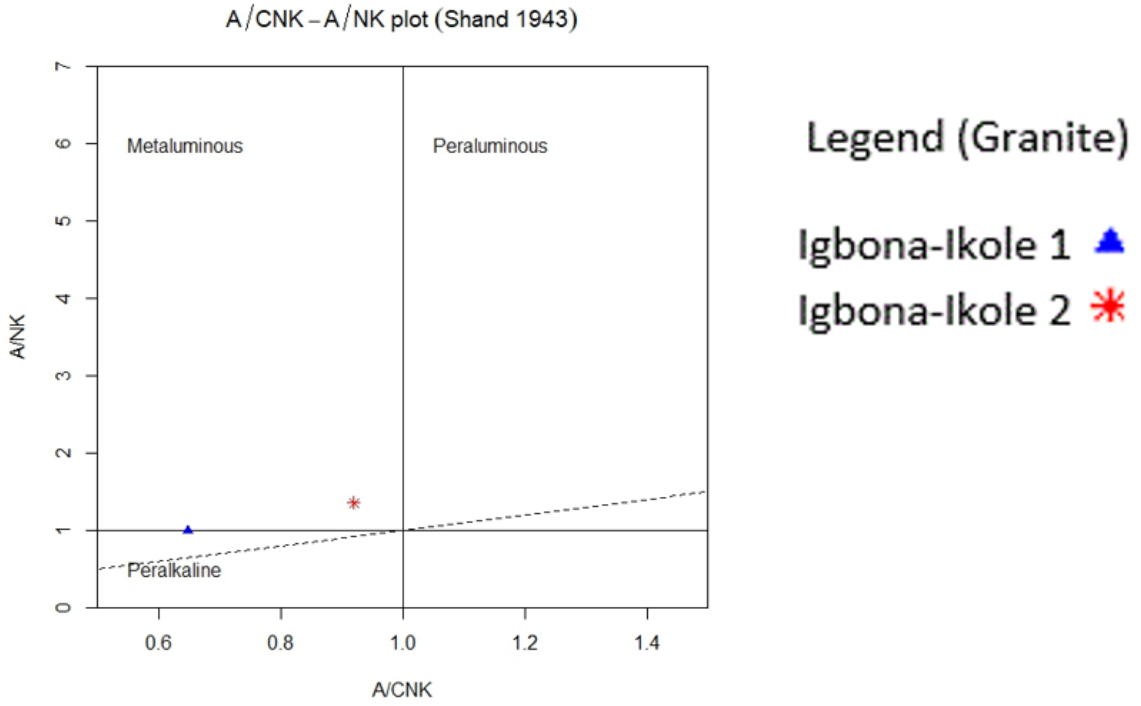

Figure 9. A/CNK–A/NK alumina saturation diagram showing the alumina saturation characteristics of the granitic rocks from the Ikole–Itapaji–Ake-Ako area. The samples plot within the **metaluminous** and **weakly peraluminous** fields, indicating evolution through fractional crystallization with limited crustal contamination (after Shand, 1943).

The Fe-number versus SiO_2 diagram Figure 10, after Frost et al. (2001**)**, classifies granitic rocks into ferroan and magnesian series based on the molecular ratio FeOt/ (FeOt + MgO**)**. This discrimination provides valuable information on the geochemical evolution, oxidation state, and tectonomagmatic affinity of granitoid magmas. The analyzed granite samples (Igbona-Ikole1 and Igbona-Ikole 2) both plot within the magnesian field**,** indicating that the granitic suite possesses a magnesian affinity.

The Igbona-ikole 2 sample plots well within the magnesian field, reflecting relatively low Fe-number values despite its high silica content. Similarly, the Igbona-Ikole 1 sample plots very close to the ferroan–magnesian discrimination boundary but remains within the magnesian field. The position of Igbona1 suggests a slight increase in iron enrichment relative to Igbona-Ikole 2; however, the sample does not cross the boundary into the ferroan field. Consequently, both samples are interpreted as belonging to the magnesian granitoid series**,** although Igbona-Ikole1 exhibits a transitional tendency toward ferroan compositions.

Magnesian granitoids are typically generated under relatively oxidizing conditions, where early crystallization of Fe–Ti oxide minerals limits iron enrichment in the residual magma. They are commonly associated with calc-alkaline magmatic suites developed in continental arc, subduction-related, and post-collisional tectonic settings. Their evolution is largely controlled by fractional crystallization of amphibole, biotite, plagioclase, and accessory oxide minerals, resulting in progressive silica enrichment without significant Fe accumulation (Shand, S. J. (1943), Frost & Frost. (2011).

The close proximity of the two granite samples on the diagram indicates that they are genetically related and most likely evolved from a common parental magma through progressive differentiation. The slightly higher Fe-number of Igbona-Ikole 1 may reflect a relatively less evolved stage of crystallization or minor variations in

ISSN No. 2321-2705 | DOI: 10.51244/IJRSI |Volume XIII Issue VII July 2026

oxidation conditions during magma evolution. Nevertheless, the overall magnesian affinity agrees well with the calc-alkaline signature observed on the AFM diagram and the metaluminous character indicated by the A/CNK–A/NK diagram, suggesting a coherent petrogenetic evolution of the granitic suite (Oyebamiji et al., 2024).

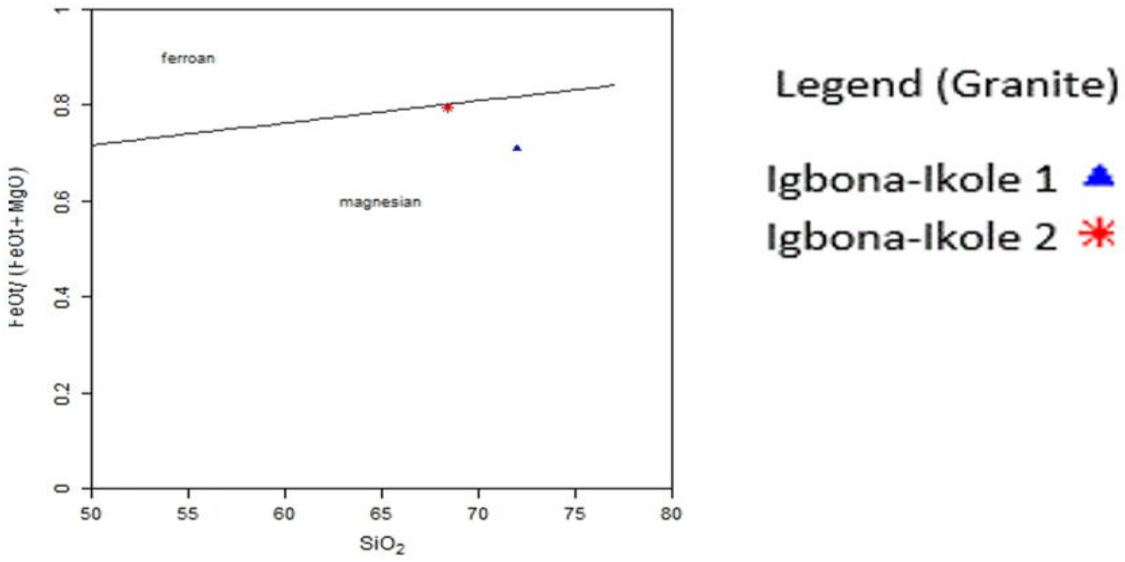

Figure 10. Fe-number (FeOt/(FeOt + MgO)) versus SiO_2 discrimination diagram after **Frost et al. (2001)** showing that the granitic rocks from the Ikole–Itapaji–Ake-Ako area plot within the **magnesian field**, indicating evolution under relatively oxidizing conditions through fractional crystallization.

Major oxides geochemistry (Granite Gneiss)

The Harker variation diagrams Figure 11 illustrate the relationships between SiO_2 and the major oxides (Al_2O_3, MgO, CaO, Na_2O, K_2O, TiO_2, P_2O_5, and FeOt) for the granite gneiss samples collected from Aba Dam 2, Ikole 3, OdoOro, Itapaji 1, Aba Dam 1, Itapaji 3, Agbeyewa Farm, Itapi/Oke-Ako, and Ake Ako 3 within the Ikole–Itapaji–Ake-Ako area. These diagrams were used to evaluate the geochemical evolution of the granite gneiss and identify the processes responsible for major-element variation during magma differentiation. The systematic distribution of the samples demonstrates progressive geochemical evolution typical of felsic calc-alkaline granitoids.

The concentrations of Al_2O_3, MgO, CaO, Na_2O, K_2O, P_2O_5, and FeOt generally decrease with increasing SiO_2. The Aba Dam 1, Itapaji 1, and OdoOro samples, which possess relatively lower silica contents (approximately 63–66 wt.% SiO_2), exhibit comparatively higher concentrations of MgO, CaO, FeOt, and TiO_2, indicating greater proportions of ferromagnesian minerals and calcic plagioclase. In contrast, the Itapi/Oke-Ako and Agbeyewa Farm samples, which possess the highest silica contents (approximately 72–74 wt.% SiO_2), display markedly lower concentrations of these oxides, reflecting progressive depletion of compatible elements through fractional crystallization (Oyebamiji et al., 2024).

The decrease in MgO and FeOt with increasing SiO_2 indicates early crystallization and removal of biotite, amphibole, and other ferromagnesian minerals from the evolving magma. Likewise, the decline in CaO suggests continued fractionation of calcic plagioclase during magma evolution. The progressive depletion of TiO_2 reflects crystallization of Fe–Ti oxide minerals such as ilmenite and magnetite, while the reduction in P_2O_5 indicates the crystallization of apatite during the later stages of differentiation (Irzon, R., 2013).

Al_2O_3 also exhibits a gradual decrease with increasing silica, indicating continuous feldspar fractionation throughout magma evolution. Although Na_2O and K_2O show slight scatter among the samples, their overall decrease with increasing SiO_2 suggests redistribution of alkali elements during feldspar crystallization and reflects the evolved felsic character of the granite gneiss. Minor (Chappell & White, 2001). deviations from

ISSN No. 2321-2705 | DOI: 10.51244/IJRSI |Volume XIII Issue VII July 2026

the overall trends are expected because the samples were collected from different outcrops that have experienced varying degrees of deformation and metamorphic overprinting.

The progressive depletion of MgO, FeOt, CaO, TiO_2, and P_2O_5, together with consistently high silica contents (approximately 62–74 wt.% SiO_2), indicates that the granite gneiss evolved through extensive fractional crystallization from a common calc-alkaline parental magma. These geochemical characteristics are typical of granitoids emplaced within continental crust during prolonged magmatic evolution and subsequently modified by regional metamorphism (Hayatu, R. A., (2024).

The Harker variation trends agree closely with the AFM diagram, which indicates calc-alkaline affinity, the TAS diagrams that classify the rocks within intermediate to felsic compositional fields, the A/CNK–A/NK diagram showing predominantly metaluminous to weakly peraluminous characteristics, and the Fe-number diagram indicating magnesian affinity. Collectively, these geochemical characteristics demonstrate that the granite gneiss samples represent differentiated felsic magmas that evolved through progressive fractional crystallization prior to regional metamorphism (Oyebamiji et al., 2024).

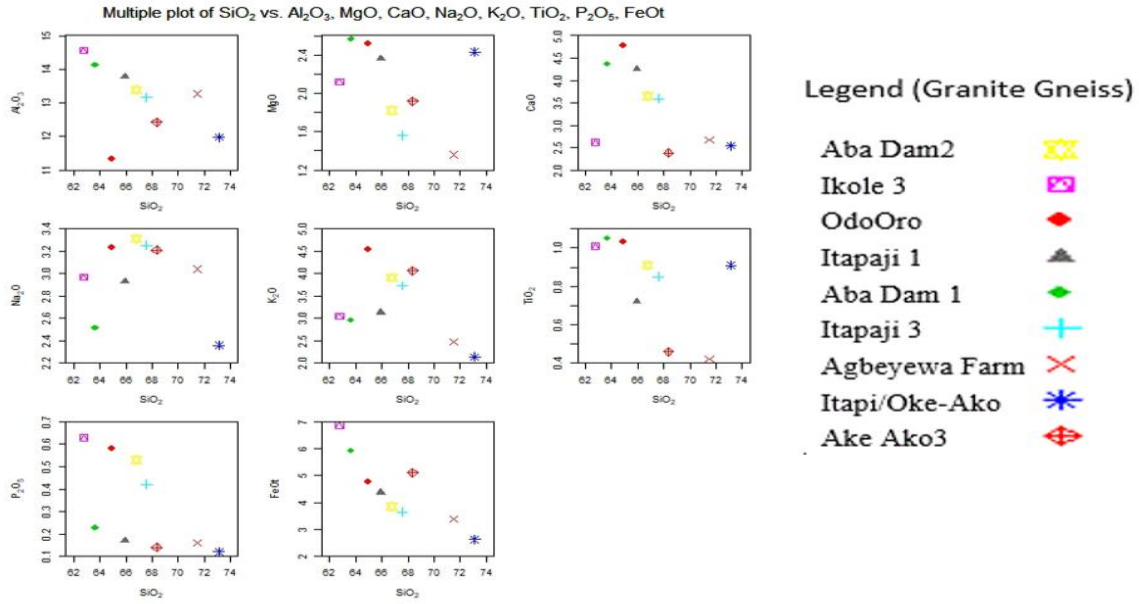

Figure 11. Harker variation diagrams showing the relationships between SiO_2 and the major oxides (Al_2O_3, MgO, CaO, Na_2O, K_2O, TiO_2, P_2O_5, and FeOt) for the granite gneisses from the Ikole–Itapaji–Ake-Ako area. The diagrams indicate systematic geochemical variations consistent with progressive fractional crystallization and magmatic differentiation (after Peccerillo & Taylor, 1976).

The A/CNK–A/NK diagram Figure 12, after Shand (1943), classifies the granite gneisses from the Ikole–Itapaji–Ake-Ako area according to their alumina saturation characteristics. The diagram distinguishes peralkaline, metaluminous, and peraluminous granitoids based on the molecular proportions of Al_2O_3, CaO, Na_2O, and K_2O. The analyzed granite gneiss samples are distributed within both the metaluminous and peraluminous fields, indicating compositional variability during magma evolution (Moyen et al., 2017).

Most of the analyzed samples, including OdoOro, Aba Dam2, Itapaji 1, Aba Dam, Itapaji 3, and Ake Ako3, plot within the metaluminous field (A/CNK < 1.0). This indicates that aluminium is adequately balanced by calcium, sodium, and potassium and is incorporated mainly into feldspars and ferromagnesian minerals. Metaluminous granitoids are typically classified as I-type granitoids and are generally derived from mantle-derived or lower crustal magmas that evolve through fractional crystallization with only limited crustal contamination (Oyebamiji et al., 2024).

In contrast, the samples from Ayewagba and Itapi/OkeA plot within the peraluminous field (A/CNK > 1.0), indicating a slight excess of aluminium relative to Ca, Na, and K. Weakly peraluminous compositions

ISSN No. 2321-2705 | DOI: 10.51244/IJRSI |Volume XIII Issue VII July 2026

commonly develop during advanced stages of magma evolution through prolonged fractional crystallization and limited assimilation of aluminous crustal materials. Such granitoids may contain aluminium-rich minerals such as muscovite, garnet, or cordierite where the degree of peraluminosity is sufficiently developed (Chappell & White, 2001).

The close distribution of the samples around the A/CNK = 1.0 boundary suggests a transitional relationship between the metaluminous and weakly peraluminous compositions. This pattern indicates that the granite gneisses most likely evolved from a common parental magma that experienced varying degrees of fractional crystallization and minor crustal interaction during emplacement. Similar transitional alumina saturation characteristics have been reported in Precambrian granitoid complexes, where progressive differentiation results in gradual shifts from metaluminous to weakly peraluminous compositions without requiring distinct magma sources (Clemens, 2003).

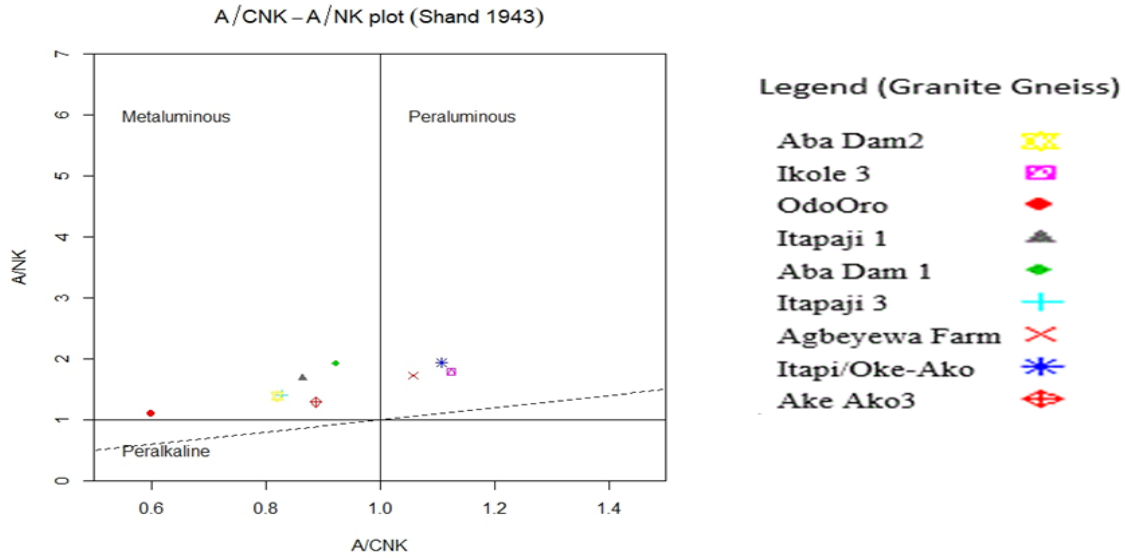

Figure 12. A/CNK–A/NK alumina saturation diagram showing that the granite gneisses from the Ikole–Itapaji–Ake-Ako area are predominantly metaluminous with a few weakly peraluminous samples, indicating evolution through fractional crystallization with minor crustal contamination (after Shand, 1943).

The Fe-number versus SiO_2 diagram Figure 13, after Frost et al., (2001), classifies the granite gneisses from the Ikole–Itapaji–Ake-Ako area into ferroan and magnesian series based on the molecular ratio FeOt/(FeOt + MgO). This classification provides important insights into the oxidation state, magmatic evolution, and tectonic affinity of granitoid rocks. The analyzed granite gneiss samples plot predominantly within the magnesian field, with one sample occurring close to the ferroan–magnesian boundary (Irzon, R., 2013).

Most of the analyzed samples, including Aba Dam2, OdoOro, Itapaji 1, Aba Dam, Itapaji 3, Ayewagba, Itapi/OkeA, and Ake Ako3, plot within the magnesian field. Their relatively low Fe-number values indicate that iron enrichment was limited during magmatic differentiation. Such compositions are characteristic of magmas that evolved under relatively oxidizing conditions, where early crystallization of Fe–Ti oxides restricted the accumulation of iron in the residual melt. Magnesian granitoids are commonly associated with calc-alkaline magmatic suites generated in continental arc and post-collisional tectonic environments (Oyebamiji et al., 2024).

The Ikole 3 sample plots very close to the ferroan–magnesian discrimination boundary but remains within the magnesian field. Its relatively higher Fe-number suggests a slight increase in iron enrichment compared with the other samples; however, it does not exhibit the geochemical characteristics of true ferroan granitoids. The position of this sample is therefore interpreted as reflecting minor compositional variation resulting from progressive fractional crystallization rather than indicating a separate magma series (Oyebamiji et al., 2024).).

The clustering of nearly all samples within the magnesian field indicates that the granite gneiss suite followed a consistent magmatic evolutionary trend. This interpretation agrees with the AFM diagram, which classifies

ISSN No. 2321-2705 | DOI: 10.51244/IJRSI |Volume XIII Issue VII July 2026

the rocks as calc-alkaline, and with the Harker variation diagrams, which demonstrate systematic depletion of FeOt, MgO, CaO, TiO_2, and P_2O_5 with increasing SiO_2. The predominantly metaluminous to weakly peraluminous compositions shown by the A/CNK–A/NK diagram further support derivation from a common parental magma that evolved primarily through fractional crystallization with only limited crustal contamination (Clemens, 2003).

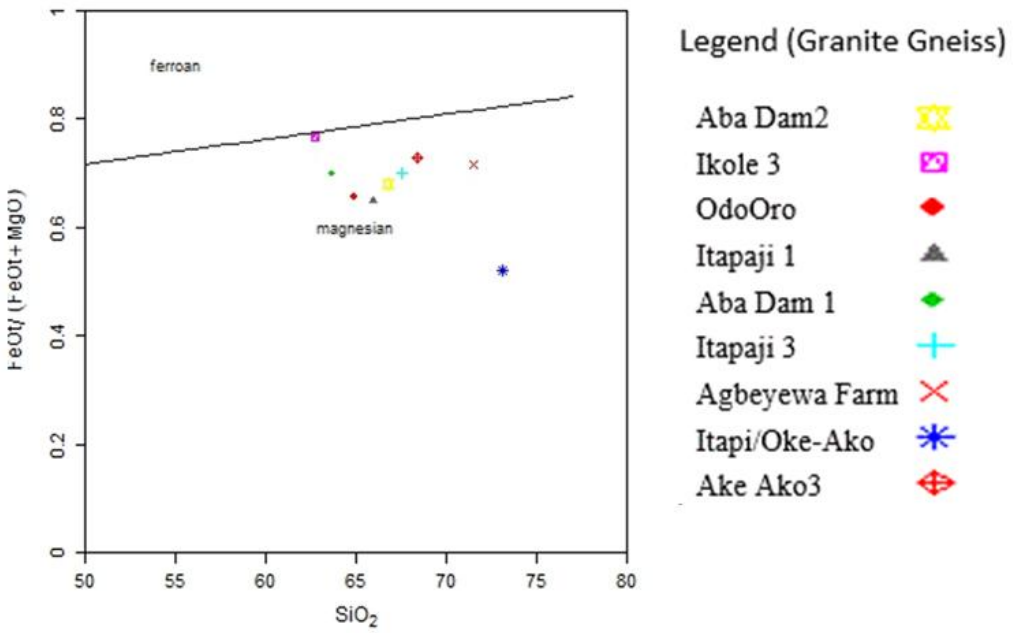

Figure 13. Fe-number (FeOt/ (FeOt + MgO)) versus SiO_2 discrimination diagram after Frost et al. (2001) showing that the granite gneisses from the Ikole–Itapaji–Ake-Ako area are predominantly magnesian, indicating evolution under relatively oxidizing conditions through progressive fractional crystallization

Major oxides geochemistry (Migmatite)

The Harker variation diagrams Figure 14 illustrate the relationships between SiO_2 and the major oxides (Al_2O_3, MgO, CaO, Na_2O, K_2O, TiO_2, P_2O_5, and FeOt) for the migmatite samples collected from Ikole 1, Ikole 2, and Ikole 4 within the Ikole–Itapaji–Ake-Ako area. These diagrams were used to evaluate the geochemical evolution of the migmatites and identify the magmatic processes responsible for the observed compositional variations. Although only three representative samples were analyzed, the diagrams reveal systematic geochemical trends that are characteristic of differentiated felsic magmas (Oyebamiji et al., 2024).

The Ikole 4 sample, which possesses the lowest silica content (approximately 55 wt.% SiO_2), exhibits the highest concentrations of Al_2O_3, MgO, CaO, Na_2O, TiO_2, and FeOt. These elevated concentrations indicate a relatively primitive composition enriched in ferromagnesian minerals, calcic plagioclase, and Fe–Ti oxide phases. Such characteristics suggest that Ikole 4 represents the least differentiated member of the migmatite suite (Moyen et, al, 2017).

In contrast, the Ikole 1 and Ikole 2 samples exhibit progressively higher SiO_2 contents (approximately 66–70 wt %), accompanied by marked decreases in MgO, CaO, TiO_2, and FeOt. These negative relationships indicate progressive fractional crystallization involving amphibole, biotite, calcic plagioclase, and Fe–Ti oxide minerals. The depletion of these compatible elements reflects continuous removal of early-crystallizing minerals from the evolving magma, resulting in progressive enrichment of silica within the residual melt (Permana et al., 2025).

Al_2O_3 also decreases slightly with increasing SiO_2, suggesting continued feldspar fractionation during magma evolution. Similarly, Na_2O exhibits a gradual decline with increasing silica, reflecting changes in plagioclase composition as differentiation progressed. In contrast, K_2O displays a positive relationship with SiO_2, with the Ikole 1 sample exhibiting the highest K_2O concentration. This enrichment reflects increasing crystallization of

ISSN No. 2321-2705 | DOI: 10.51244/IJRSI |Volume XIII Issue VII July 2026

K-feldspar during the later stages of magma evolution and is characteristic of evolved felsic magmas (Frost & Frost 2011).

The behaviour of P_2O_5 differs slightly from the other compatible oxides. The concentration increases from Ikole 4 to Ikole 1 before declining slightly in Ikole 2, suggesting temporary enrichment of phosphorus in the residual melt before apatite crystallization. Such behaviour is commonly observed during the late stages of felsic magma differentiation, when incompatible elements become concentrated before accessory mineral saturation (Barbarin, (1999).

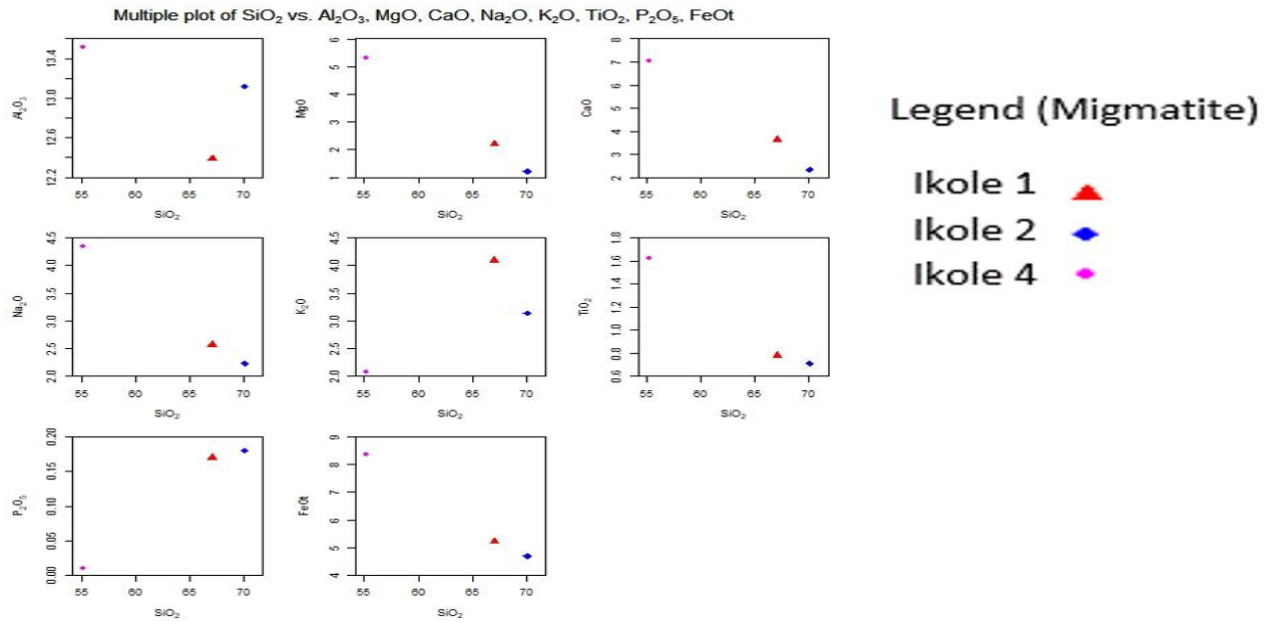

Figure 14. Harker variation diagrams showing the relationships between SiO_2 and the major oxides (Al_2O_3, MgO, CaO, Na_2O, K_2O, TiO_2, P_2O_5, and FeOt) for the migmatites from the Ikole–Itapaji–Ake-Ako area. The observed geochemical variations indicate progressive fractional crystallization and magmatic differentiation (after Peccerillo & Taylor, 1976).

The A/CNK–A/NK diagram Figure 15, after Shand (1943), classifies the migmatites from the Ikole–Itapaji–Ake-Ako area according to their alumina saturation characteristics using the molecular proportions of Al_2O_3, CaO, Na_2O, and K_2O. The diagram distinguishes peralkaline, metaluminous, and peraluminous granitoids and provides important information on magma source characteristics and the degree of crustal involvement during magma evolution. The analyzed migmatite samples are distributed within both the metaluminous and peraluminous fields, indicating slight compositional variation within the suite.

The Ikole 1 and Ikole 4 samples plot within the metaluminous field (A/CNK < 1.0), indicating that aluminium is balanced by calcium, sodium, and potassium and is mainly accommodated within feldspars and ferromagnesian minerals. Metaluminous compositions are characteristic of I-type granitoids and are generally interpreted to originate from mantle-derived or lower crustal magmas that evolve primarily through fractional crystallization with limited crustal contamination (Clemens, 2003).

In contrast, the Ikole 2 sample plots within the peraluminous field (A/CNK > 1.0), indicating a slight excess of aluminium relative to Ca, Na, and K. This weakly peraluminous character suggests a greater contribution from crustal materials, probably through partial melting of aluminous continental crust or limited assimilation during magma evolution. Weakly peraluminous granitoids commonly develop during advanced stages of magmatic differentiation and may contain aluminium-rich minerals where sufficient aluminium is available (Hayatu, 2024**).**

ISSN No. 2321-2705 | DOI: 10.51244/IJRSI |Volume XIII Issue VII July 2026

The occurrence of both metaluminous and weakly peraluminous compositions indicates that the migmatites were derived from a genetically related magma that experienced variable degrees of differentiation and crustal interaction. The proximity of the samples to the metaluminous–peraluminous boundary suggests that the transition in alumina saturation was gradual rather than abrupt, reflecting progressive magmatic evolution accompanied by localized crustal reworking during high-grade metamorphism (Chappell, B. W., & White, A. J. R. 2001).

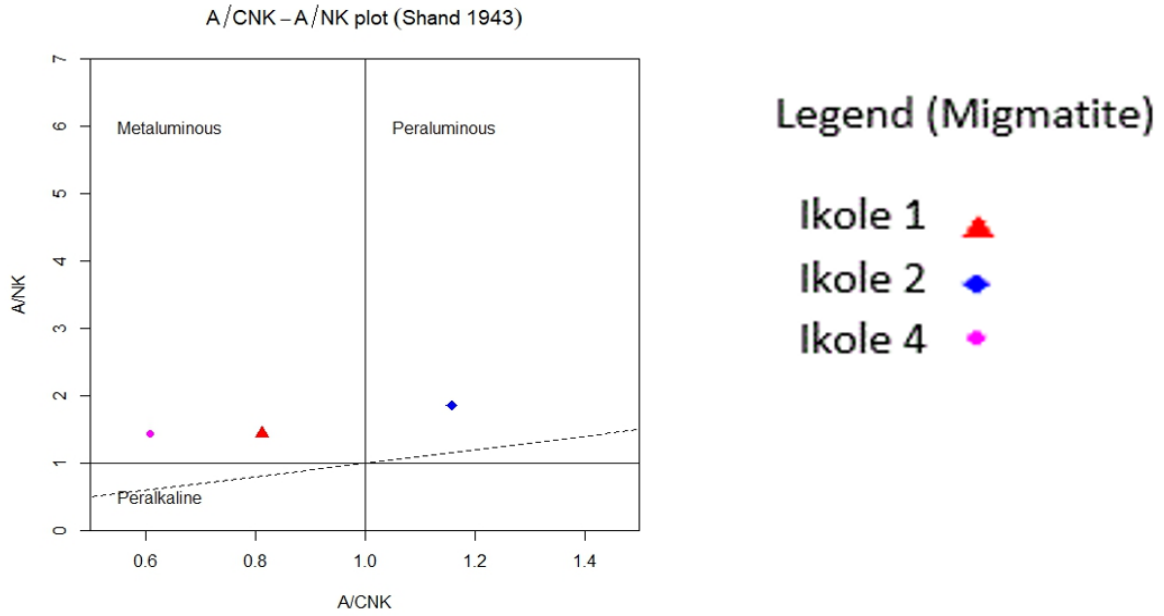

Figure 15. A/CNK–A/NK alumina saturation diagram showing that the migmatites from the Ikole–Itapaji–Ake-Ako area are predominantly metaluminous with one weakly peraluminous sample, indicating evolution through fractional crystallization accompanied by limited crustal contamination (after Shand, 1943).

The Fe-number versus SiO_2 diagram Figure 16, after Frost et al. (2001), classifies the migmatites from the Ikole–Itapaji–Ake-Ako area into ferroan and magnesian series based on the molecular ratio FeOt/(FeOt + MgO). This classification provides valuable information on the oxidation state, magmatic evolution, and tectonomagmatic affinity of granitoid rocks. The analyzed migmatite samples all plot within the magnesian field, indicating that the migmatitic suite possesses a consistent magnesian affinity.

The Ikole 1 sample occupies the central part of the magnesian field, indicating relatively low iron enrichment despite its felsic composition. Similarly, the Ikole 4 sample plots well within the magnesian field and exhibits the lowest Fe-number among the analyzed samples, reflecting crystallization under relatively oxidizing conditions where iron enrichment was effectively suppressed. The Ikole 2 sample plots very close to the ferroan–magnesian discrimination boundary but remains within the magnesian field. Although this sample exhibits a comparatively higher Fe-number, it does not cross into the ferroan field and therefore retains a magnesian character (Clemens, J. D., 2003).

The predominance of magnesian compositions indicates that the parental magma evolved under oxidizing conditions, where early crystallization of Fe–Ti oxide minerals limited the accumulation of iron within the residual melt. Such magnesian granitoids are characteristic of calc-alkaline magmatic suites emplaced in continental arc and post-collisional tectonic environments. Their evolution is commonly controlled by progressive fractional crystallization involving amphibole, biotite, plagioclase, and accessory oxide minerals, resulting in silica enrichment without significant iron enrichment (Barbarin, B. (1999).

The close clustering of the three samples within the magnesian field suggests that the migmatites were derived from a common parental magma and experienced similar geochemical evolution despite minor compositional differences. This interpretation agrees with the AFM diagram, which indicates predominantly calc-alkaline

ISSN No. 2321-2705 | DOI: 10.51244/IJRSI |Volume XIII Issue VII July 2026

affinity, the Harker variation diagrams showing systematic fractional crystallization trends, and the A/CNK–A/NK diagram, which indicates predominantly metaluminous compositions with minor peraluminous characteristics. Likewise, the R_1–R_2 tectonic discrimination diagram supports emplacement during syn- to post-collisional tectonic evolution (Moyen et al, 2017).

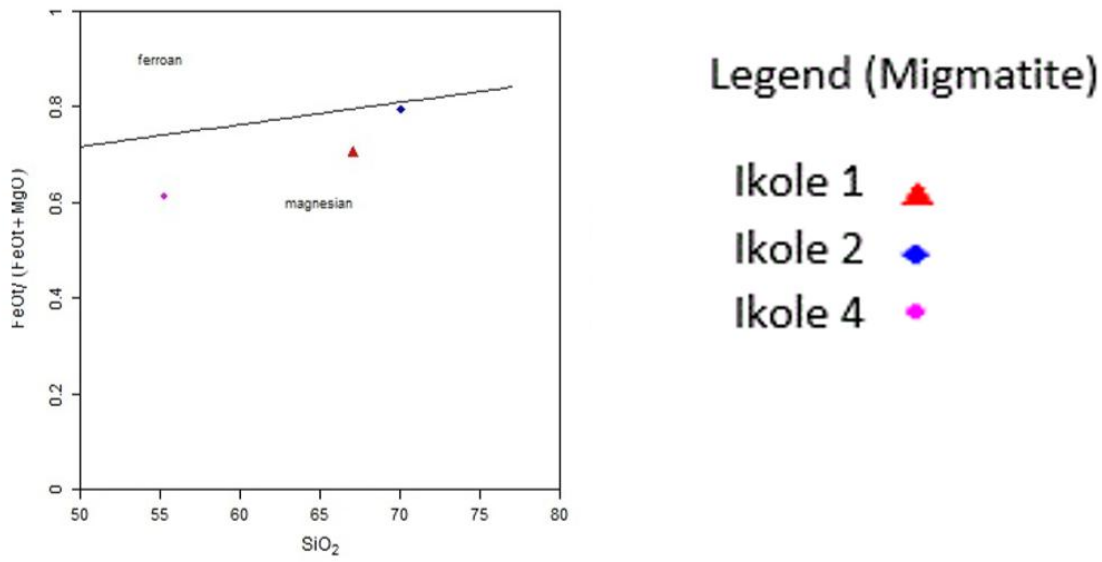

Figure 16. Fe-number (FeOt/(FeOt + MgO)) versus SiO_2 discrimination diagram after Frost et al. (2001) showing that the migmatites from the Ikole–Itapaji–Ake-Ako area plot within the magnesian field, indicating evolution under relatively oxidizing conditions through progressive fractional crystallization.

Major oxides geochemistry (Pegmatite)

The Harker variation diagrams Figure 17 illustrate the relationships between SiO_2 and the major oxides (Al_2O_3, MgO, CaO, Na_2O, K_2O, TiO_2, P_2O_5, and FeOt) for the pegmatite samples collected from Aba Farm Itapaji, Itapaji 2, Omu, and Ake Ako 2 within the Ikole–Itapaji–Ake-Ako area. These diagrams were used to evaluate the geochemical evolution of the pegmatites and identify the major-element trends associated with magma differentiation. The systematic variation of the samples reflects the evolution of highly differentiated felsic magmas.

The Omu sample, which has the lowest SiO_2 content (approximately 69 wt.%), exhibits the highest concentrations of MgO, CaO, TiO_2, and FeOt. These elevated values indicate that Omu represents the least evolved pegmatite within the suite and retains relatively greater proportions of ferromagnesian minerals, calcic plagioclase, and Fe–Ti oxide phases. In contrast, the Aba Farm Itapaji sample, with the highest SiO_2 content (approximately 76 wt.%), displays the lowest concentrations of FeOt and TiO_2, reflecting advanced fractional crystallization and progressive depletion of compatible elements (Chappell & White, 2001).

The concentrations of MgO, CaO, TiO_2, and FeOt generally decrease with increasing SiO_2. These negative relationships indicate early crystallization and removal of amphibole, biotite, calcic plagioclase, and Fe–Ti oxide minerals during magma evolution. Likewise, the gradual depletion of CaO reflects continuous fractionation of calcic plagioclase, while decreasing TiO_2 suggests crystallization of ilmenite and magnetite during the intermediate stages of differentiation (Moyen et al., 2017).

Al_2O_3 shows a slight overall decrease with increasing SiO_2, indicating progressive feldspar fractionation during the evolution of the pegmatitic melt. Similarly, Na_2O exhibits a gradual decline as silica increases, suggesting compositional evolution of plagioclase feldspar. K_2O displays only minor variation among the samples but remains consistently high, reflecting the abundance of K-feldspar and muscovite that characterize highly evolved granitic pegmatites. The elevated alkali contents are typical of residual felsic melts produced during advanced stages of magmatic differentiation (Barbarin, 1999).

ISSN No. 2321-2705 | DOI: 10.51244/IJRSI |Volume XIII Issue VII July 2026

The behaviour of P_2O_5 differs slightly from the other compatible oxides. Higher concentrations occur in the Itapaji 2 and Ake Ako 2 samples, whereas the Omu sample contains the lowest concentration. This variation suggests temporary enrichment of phosphorus in the residual melt before apatite crystallization, a common feature of highly fractionated granitic pegmatite systems (Moyen et al., 2017).

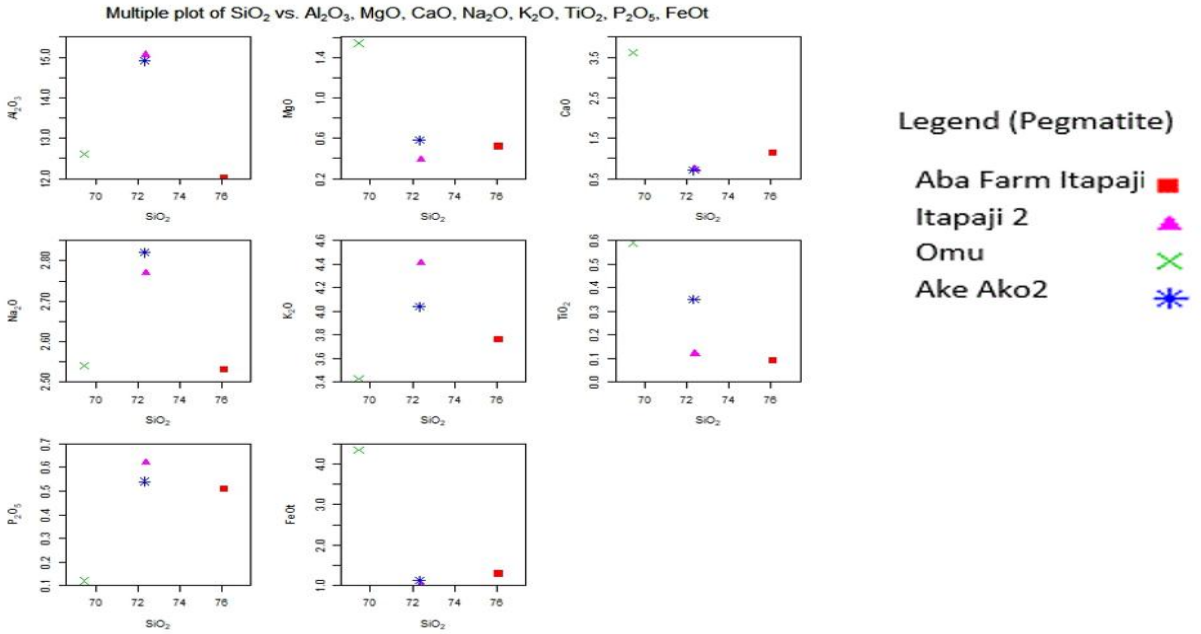

Figure 17. Harker variation diagrams showing the relationships between SiO_2 and the major oxides (Al_2O_3, MgO, CaO, Na_2O, K_2O, TiO_2, P_2O_5, and FeOt) for the pegmatites from the Ikole–Itapaji–Ake-Ako area. The geochemical trends indicate advanced fractional crystallization and the evolution of highly differentiated felsic magmas (after Peccerillo & Taylor, 1976).

The A/CNK–A/NK diagram Figure 18, after Shand (1943), was used to determine the aluminium saturation characteristics of the pegmatite samples collected from Aba Farm Itapaji, Itapaji 2, Omu, and Ake Ako 2 within the Ikole–Itapaji–Ake-Ako area. The diagram distinguishes peralkaline, metaluminous, and peraluminous rocks based on the relative proportions of Al_2O_3, CaO, Na_2O, and K_2O. The distribution of the samples indicates that the pegmatites are predominantly peraluminous, with one sample exhibiting a metaluminous composition.

The Omu sample plots within the metaluminous field, with an A/CNK value of less than 1.0 and an A/NK value greater than 1.0. This position indicates that aluminium is balanced by alkali and alkaline-earth elements and suggests crystallization from a relatively less evolved felsic magma. Metaluminous compositions are commonly associated with I-type granitic magmas derived from igneous protoliths and characterized by relatively abundant feldspar and hornblende (Moyen et al., 2023).

In contrast, the Aba Farm Itapaji, Itapaji 2, and Ake Ako 2 samples plot within the peraluminous field, having A/CNK values greater than 1.0 and A/NK values exceeding 1.0. These samples indicate an excess of aluminium relative to CaO, Na_2O, and K_2O, suggesting enrichment in aluminous minerals such as muscovite, biotite, and accessory phases. The peraluminous character reflects advanced magmatic differentiation and is typical of highly evolved pegmatitic melts generated during the late stages of granite evolution (Frost & Frost, 2011).

Among the peraluminous samples, Ake Ako 2 exhibits the highest A/CNK value, indicating the greatest degree of aluminium saturation within the pegmatite suite. Itapaji 2 occupies an intermediate position, whereas Aba Farm Itapaji is only weakly peraluminous. These variations suggest progressive enrichment of aluminium in the residual melt during fractional crystallization, resulting in increasingly evolved pegmatitic compositions (Barbarin, 1999).

ISSN No. 2321-2705 | DOI: 10.51244/IJRSI |Volume XIII Issue VII July 2026

None of the samples plot within the peralkaline field, indicating that alkali enrichment never exceeded aluminium saturation during magma evolution. This absence of peralkaline compositions confirms that the pegmatites evolved under calc-alkaline conditions rather than alkaline magmatic conditions. The predominance of peraluminous compositions is consistent with pegmatites generated from highly fractionated granitic magmas emplaced within continental crust (Clemens, 2003).

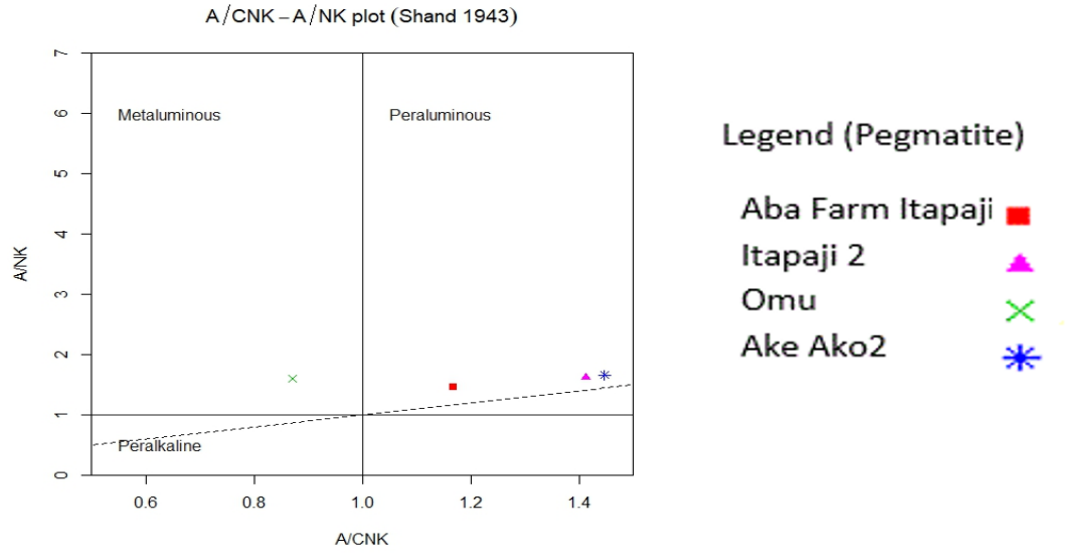

Figure 18. A/CNK–A/NK alumina saturation diagram showing that the pegmatites from the Ikole–Itapaji–Ake-Ako area are predominantly peraluminous, with one metaluminous sample, indicating derivation from highly evolved felsic magmas through extensive fractional crystallization and crustal interaction (after Shand, 1943).

Trace elements geochemistry

The results of the factor analysis presented in Table 1 and Figure 19 reveal two statistically significant components that collectively explain 92.04% of the total geochemical variance within the study area. Component 1 has an eigenvalue (EV) of 8.034 and accounts for 80.34% of the total variance, whereas Component 2 has an eigenvalue of 1.171 and contributes an additional 11.71%. The cumulative variance (CVAR) of 92.04% indicates that the two extracted components adequately explain the elemental associations and geochemical variability of the study area. According to the Kaiser criterion, components with eigenvalues greater than one are considered significant; therefore, both extracted components are interpreted as representing the principal geochemical processes controlling elemental distribution and mineralization (Rollinson, 1993). Component 1 is interpreted as the lithological factor because it reflects the primary geochemical signature inherited from the host rocks, whereas Component 2 represents the pathfinder factor, highlighting elements associated with hydrothermal alteration and mineral exploration.

Table 1 shows that Component 1 is characterized by very strong positive loadings for Cu (0.966), Ni (0.983), Co (0.951), Fe (0.939), Zn (0.863), and Mn (0.849). These high factor loadings indicate that the elements are strongly correlated and probably originated from a common geochemical source. Copper, nickel, cobalt, iron, zinc, and manganese are commonly associated with mafic to intermediate lithologies and sulphide-bearing mineral assemblages. Their strong association suggests that Component 1 represents the lithological factor, reflecting the primary geochemical composition of the basement rocks inherited from magmatic differentiation and subsequent geological evolution. The enrichment of these elements is further influenced by structurally controlled hydrothermal processes, whereby hydrothermal fluids migrated along fractures, shear zones, and lithological contacts, resulting in localized sulphide mineralization within the basement complex (Moyen et al., 2017).

Component 2 is dominated by arsenic (As = 0.728), thorium (Th = 0.356), silver (Ag = 0.224), and a very weak contribution from lead (Pb = 0.008). Although the loadings of Ag, Th, and Pb are comparatively lower

ISSN No. 2321-2705 | DOI: 10.51244/IJRSI |Volume XIII Issue VII July 2026

than those of Component 1, their association suggests a secondary geochemical process related to hydrothermal alteration and accessory mineral concentration. Component 2 is therefore interpreted as the pathfinder factor because arsenic is widely recognized as a pathfinder element in hydrothermal mineral exploration, while thorium is commonly concentrated in accessory minerals such as monazite, allanite, and zircon. Silver and lead further complement this association, indicating late-stage hydrothermal activity and fluid–rock interaction that may accompany metallic mineralization (Verma & Agrawal, 2011).

The communality values further demonstrate the robustness of the factor model. Most elements exhibit exceptionally high communalities, ranging from 0.773 for Mn to 0.998 for Cu. Copper (0.998), Co (0.997), Ni (0.967), Ag (0.963), Zn (0.958), Pb (0.956), Fe (0.921), Th (0.863), As (0.809), and Mn (0.773) all possess values exceeding 0.77, indicating that more than 77% of the variability of each element is explained by the two extracted components. These high communalities confirm that the factor solution adequately represents the original geochemical dataset and that very little unexplained variance remains (Frost et al., 2001).

The graphical representation in Figure 19 clearly supports the numerical results presented in Table 1. The chart illustrates the dominance of Component 1 over Component 2 through consistently high loading values for Cu, Zn, Ni, Co, Mn, and Fe. It also highlights the markedly larger eigenvalue of Component 1 (8.034) compared to Component 2 (1.171), confirming that the first component exerts the greatest influence on the geochemical dataset. Likewise, the chart demonstrates the high communality values for nearly all elements, showing that the extracted components effectively account for the observed elemental variability. The pronounced difference between the percentage variance explained by Component 1 (80.34%) and Component 2 (11.71%) further emphasizes that the lithological factor is the dominant control on elemental distribution, whereas the pathfinder factor reflects subordinate hydrothermal processes.

The factor analysis demonstrates that the Cu–Ni–Co–Fe–Zn–Mn association constitutes the dominant lithological factor within the study area, reflecting the primary geochemical characteristics of the basement rocks, whereas the As–Th–Ag–Pb association represents the pathfinder factor, indicating hydrothermal alteration and potential zones of mineralization. The excellent cumulative variance of 92.04% indicates that the extracted components successfully summarize the geochemical behaviour of the analysed elements and provide a reliable basis for identifying mineralization controls. These findings suggest that metallic mineralization within the study area is principally controlled by magmatic–hydrothermal processes superimposed on favourable basement lithologies, with pathfinder elements serving as useful indicators of hydrothermal alteration and prospective mineralized zones (Rose et al., 1979; Frost et al., 2001).

Table 1. Results of factor analysis showing the extracted principal components, corresponding factor loadings, and the percentage of variance explained by each component. The analysis identifies the major geochemical associations and underlying processes controlling elemental distribution and mineralization patterns within the study area.

Variables	Comp1	Comp2	Communality
Cu	.966		.998
Pb		.008	.956
Zn	.863		.958
Ag		.224	.963
Ni	.983		.967
Co	.951		.997
Mn	.849		.773

ISSN No. 2321-2705 | DOI: 10.51244/IJRSI |Volume XIII Issue VII July 2026

Fe	.939		.921
As		.728	.809
Th		.356	.863
EV	8.034	1.171	
VAR%	80.34%	11.71%	
CVAR%	80.34%	92.044%	

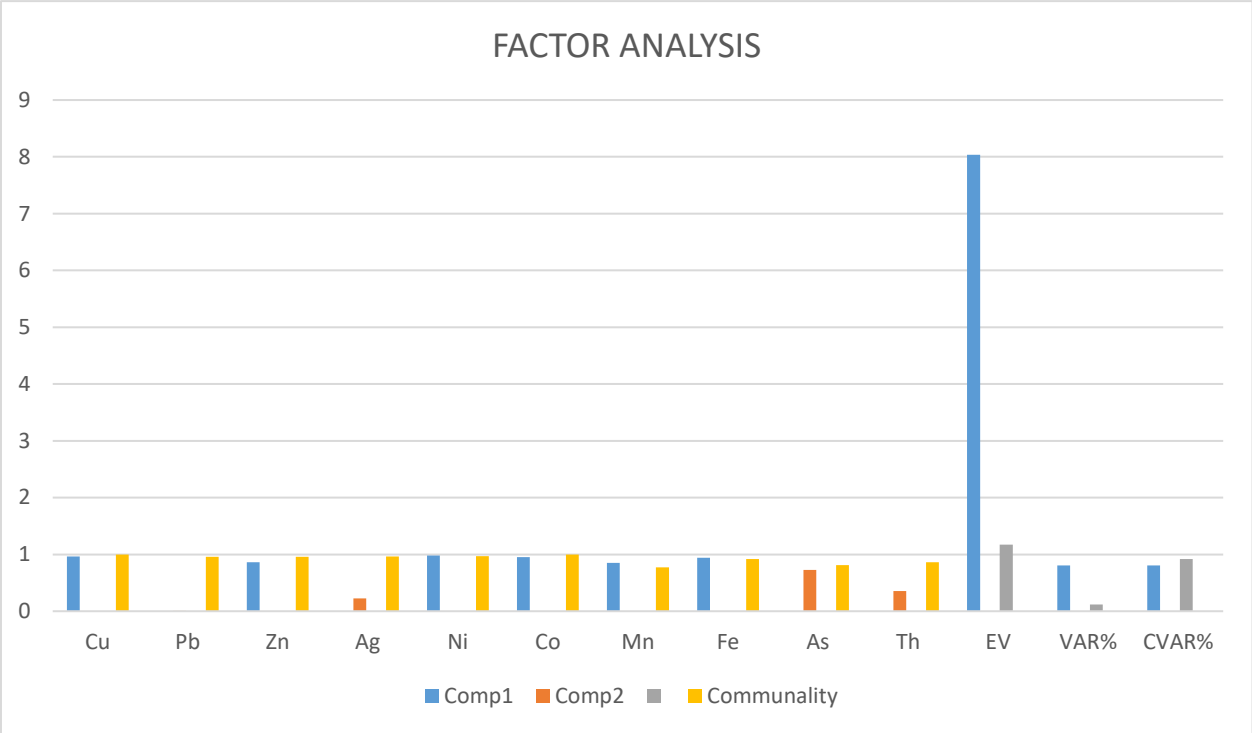

Figure 19. Factor analysis chart showing the loadings of Components 1 and 2, communalities, eigenvalues (EV), percentage variance explained (VAR%), and cumulative variance (CVAR%) for the analysed geochemical elements. The chart illustrates the dominance of Component 1 in controlling the geochemical variability and mineralization patterns within the study area.

The correlation coefficient matrix (Table 2) and the corresponding chart (Figure 20) reveal significant relationships among the analyzed trace elements, reflecting their geochemical behavior and possible mineralization processes. Strong positive correlations occur between Cu–Ni (r = 0.845), Cu–Co (r = 0.824), Cu–Fe (r = 0.804), Ni–Co (r = 0.935), Ni–Fe (r = 0.917), and Co–Fe (r = 0.876), indicating a common lithological source and similar geochemical affinity, likely related to mafic mineral assemblages and hydrothermal enrichment. Zn also exhibits moderate to strong positive correlations with Cu (r = 0.606), Ni (r = 0.596), Co (r = 0.683), and Fe (r = 0.529), suggesting its association with the same mineralizing system (Olade, 2020).

Conversely, Ag shows strong negative correlations with Cu (r = –0.858), Ni (r = –0.914), Co (r = –0.849), and Fe (r = –0.890), but a strong positive relationship with Pb (r = 0.913) and Th (r = 0.829), indicating that Ag is controlled by a different geochemical process or mineral phase. Similarly, Pb exhibits strong positive correlations with Th (r = 0.891) and moderate positive correlation with As (r = 0.500), suggesting enrichment within felsic or hydrothermal environments (Odewumi & Olarewaju, 2013).

Mn and As generally display weak or insignificant correlations with most elements, implying independent geochemical behavior and limited influence on the principal mineralization processes. As illustrated in Figure

ISSN No. 2321-2705 | DOI: 10.51244/IJRSI |Volume XIII Issue VII July 2026

20**,** the chart highlights the predominance of strong positive correlations among Cu, Ni, Co, Fe, and Zn, while Ag and Pb exhibit contrasting relationships. Collectively, these results indicate at least two distinct geochemical associations: a Cu–Ni–Co–Fe–Zn mineralization suite and a Pb–Ag–Th association, reflecting multiple sources and mineralizing events within the study area (Rahman et al., 2024; Oladejo & Akinyemi, 2024; Nnoli et al., 2025).

Table 2. Correlation coefficient matrix showing the degree and direction of relationships among the analyzed geochemical elements. Positive and negative correlation values indicate possible common sources, mineral associations, and geochemical processes influencing elemental distribution. The matrix provides a basis for interpreting elemental affinities and assessing mineralization potential within the study area.

	Cu	Pb	Zn	Ag	Ni	Co	Mn	Fe	As	Th
Cu	1									
Pb	-.543**	1								
Zn	.606**	-.424*	1							
Ag	-.858*	.913*	-0.7598	1						
Ni	.845**	-.496*	.596**	-.914*	1					
Co	.824**	-.557**	.683**	-.849*	.935**	1				
Mn	-0.294	-0.1273	0.20883	-.820*	-0.3365	-0.281	1			
Fe	.804**	-.710**	.529**	-.890*	.917**	.876**	-0.2066	1		
As	-0.176	.500*	-0.0909	0.75	-0.1921	-0.0929	0.00011	-.401*	1	
Th	-.506*	.891**	-.407*	.829*	-.493*	-.460*	-0.1191	-.700**	.636**	1

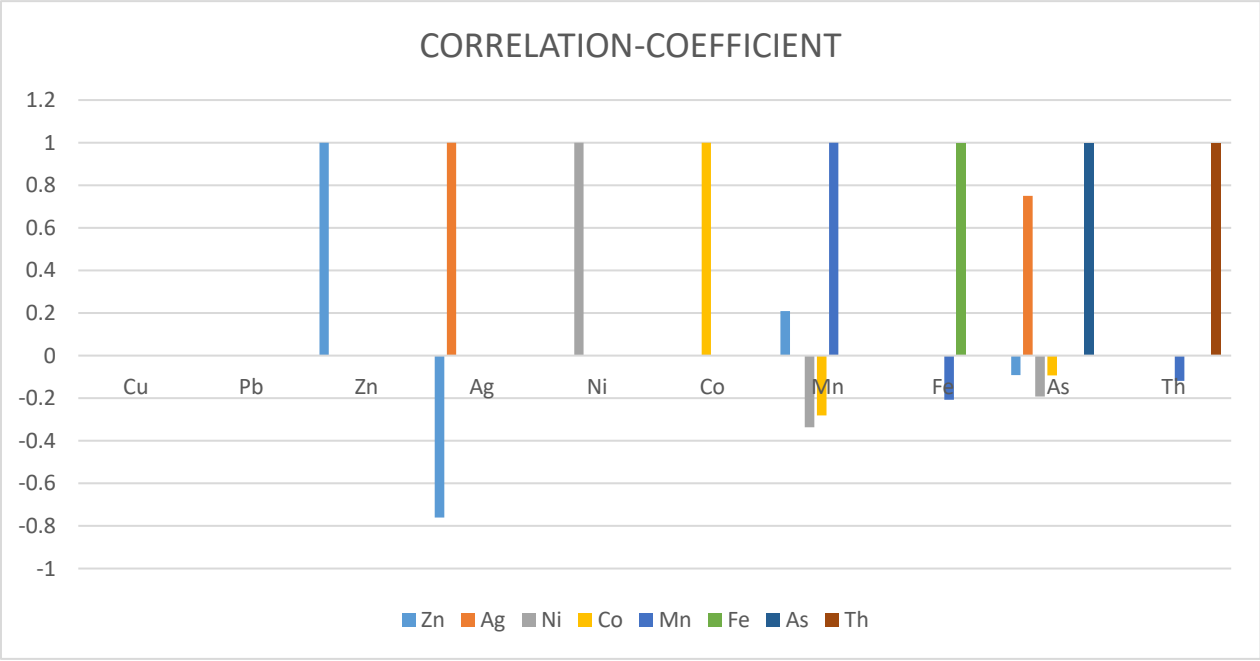

Figure 20. Correlation coefficient chart illustrating the strength and direction of relationships among the analyzed trace elements. The chart highlights positive and negative elemental associations that reflect common geochemical sources, mineral assemblages, and mineralization processes within the study area.

ISSN No. 2321-2705 | DOI: 10.51244/IJRSI |Volume XIII Issue VII July 2026

Integration of Major and Trace Elements Geochemistry

The integration of the major- and trace-element geochemical data indicates that the basement rocks of the Ikole–Itapaji–Ake-Ako area evolved through progressive magmatic differentiation, with fractional crystallization playing a dominant role in their petrogenesis. The Harker variation diagrams show systematic depletion of MgO, FeOt, CaO, and TiO_2 with increasing SiO_2, reflecting the early crystallization and removal of ferromagnesian minerals, plagioclase, and Fe–Ti oxides during magma evolution (Rollinson, 1993; Frost et al., 2001). The predominance of metaluminous to weakly peraluminous compositions on the A/CNK–A/NK diagram and the mainly magnesian affinity indicated by the Fe-number discrimination diagram further suggest derivation from genetically related calc-alkaline magmas with only minor crustal contamination.

The trace-element data complement these observations. Factor analysis identifies a dominant Cu–Ni–Co–Fe–Zn association, indicating a common magmatic-hydrothermal source, while the Pb–Ag–Th–As association reflects secondary lithological and hydrothermal processes. Similarly, the correlation coefficient matrix reveals strong positive relationships among Cu, Ni, Co, Fe, and Zn, confirming their genetic association, whereas Pb and Ag exhibit contrasting behaviour, suggesting a separate stage of elemental enrichment (Rose et al., 1979; Olade, 2020).

Overall, the combined major- and trace-element evidence indicates that the basement rocks were generated from compositionally related magmas that evolved mainly through fractional crystallization and were subsequently modified by structurally controlled hydrothermal activity. These processes collectively controlled the distribution of the trace elements and contributed to the mineralization potential of the Ikole–Itapaji–Ake-Ako area.

Study Limitations

This study was limited by the relatively small number of representative samples selected for whole-rock geochemical analysis, which may not fully capture the complete geochemical variability of all lithological units within the study area. The interpretation of major-element geochemistry was based primarily on Harker variation diagrams, the A/CNK–A/NK alumina saturation diagram, and the Fe-number discrimination diagram, while trace-element interpretation relied on factor analysis and correlation coefficient analysis. Consequently, more advanced geochemical discrimination methods, rare earth element (REE) data, and isotopic analyses were not included. Nevertheless, the integration of field geological observations with major- and trace-element geochemistry provides a reliable basis for interpreting the petrogenesis, magmatic evolution, and mineralization potential of the crystalline rocks within the Ikole–Itapaji–Ake-Ako area.

CONCLUSION

This study integrated geological mapping with major- and trace-element geochemistry to investigate the petrogenesis and mineralization potential of the crystalline rocks within the Ikole–Itapaji–Ake-Ako area, southwestern Nigeria. Geological mapping revealed that the area is underlain predominantly by migmatite, granite gneiss, granite, charnockite, and pegmatite, with structural features such as fractures, joints, and foliations that provide favourable pathways for hydrothermal fluid circulation and mineralization.

Major-element geochemical results indicate that the various lithological units evolved predominantly through fractional crystallization, as demonstrated by the systematic Harker variation trends. The A/CNK–A/NK alumina saturation diagram shows that the rocks range from metaluminous to weakly peraluminous compositions, reflecting limited crustal contamination during magma evolution. Likewise, the Fe-number discrimination diagram indicates that most of the rocks belong to the magnesian granitoid series, with only minor transitional ferroan characteristics observed in a few samples, suggesting crystallization under relatively oxidizing conditions.

Trace-element statistical analyses further revealed distinct geochemical associations within the study area. Factor analysis identified Cu–Ni–Co–Fe–Zn as the dominant mineralization association, whereas As–Th–Ag–Pb constitute a secondary geochemical assemblage related to lithological variation and hydrothermal

alteration. The strong positive correlations among Cu, Ni, Co, Fe, and Zn indicate a common geochemical source and support the occurrence of structurally controlled magmatic–hydrothermal mineralization.

Overall, the integrated geological and geochemical evidence indicates that the Ikole–Itapaji–Ake-Ako area possesses favourable geological conditions for metallic mineralization. The study demonstrates that major- and trace-element geochemistry provides valuable information for understanding magma evolution, petrogenesis, and mineralization potential within the Precambrian Basement Complex of southwestern Nigeria.

RECOMMENDATIONS

1. More detailed geochemical investigations involving rare earth elements (REEs), isotopic analyses, and additional trace-element data should be carried out to further constrain the petrogenesis and source characteristics of the crystalline rocks.

2. Detailed structural mapping and integrated geophysical surveys should be undertaken to delineate subsurface structures and identify zones of hydrothermal alteration that may host economically significant mineralization.

3. A larger number of representative rock samples should be analyzed to improve the geochemical database and better characterize the spatial variability of the different lithological units.

4. Follow-up exploration, including detailed geochemical sampling, trenching, and exploratory drilling, is recommended in areas exhibiting strong Cu–Ni–Co–Fe–Zn geochemical associations to evaluate their economic mineral potential.

5. The integrated geological and geochemical approach adopted in this study should be applied to adjacent parts of the Nigerian Basement Complex to improve regional mineral exploration and resource assessment.

Declaration of competing interests

Ethical Approval

This study did not involve human participants, animals, or any form of clinical or ethical experimentation. Therefore, formal ethical approval was **not required.**

Declaration of generative AI and AI-assisted technologies in the manuscript preparation process

During the preparation of this work, the authors used ChatGPT (GPT-5-mini) to assist with language editing and content organization. After using this tool, the authors reviewed, revised, and verified all content to ensure accuracy, originality, and authenticity, and take full responsibility for the content of the published article.

Consent to Participate

s no human participants were involved in this research, obtaining consent for participation was **not applicable.** All research activities adhered to standard field and laboratory protocols without the involvement of people.

Consent to Publish

This study does not include any personal, sensitive, or identifiable information. Consequently, consent to publish was **not applicable**. All data presented are **scientific observations and analyses**, fully anonymized, and pose no ethical concerns.

Availability of Data and Materials:

The datasets used and analyzed during this study are available from the corresponding author upon reasonable request.

Authors' Contributions

Adeleke Ojo conceived and designed the study, carried out the geological field investigations, collected rock samples, performed the geochemical data analysis and interpretation, prepared the figures and tables, and drafted the manuscript. **Olusola Amos OlaOlorun** supervised the research, provided methodological guidance, contributed to the interpretation of the geological and geochemical results, critically reviewed the manuscript for important intellectual content, and approved the final version of the manuscript. Both authors read and approved the final manuscript.

REFERENCES

1. Adetunla, F. R., Ayodele, O. S., Asowata, I. T., & Olususi, J. (2025). Integrated geological, aeromagnetic, and remote sensing datasets in litho-structural mapping of basement rocks in southwestern Nigeria. Asian Journal of Geological Research, 8(3), 523–553. https://doi.org/10.9734/ajoger/2025/v8i3213
2. Ajibade, A. C., Woakes, M., & Rahaman, M. A. (1987). Proterozoic crustal development in the Pan-African regime of Nigeria. In A. Kröner (Ed.), Proterozoic Lithospheric Evolution (Geodynamics Series, Vol. 17, pp. 259–271). Washington, DC: American Geophysical Union. https://agupubs.onlinelibrary.wiley.com/doi/10.1029/GD017p0259
3. Barbarin, B. (1999). A review of the relationships between granitoid types, their origins and their geodynamic environments. Lithos, 46(3), 605–626. DOI: https://doi.org/10.1016/S0024-4937(98)00085-1 https://www.sciencedirect.com/science/article/pii/S0024493798000851
4. Chappell, B. W., & White, A. J. R. (2001). Two contrasting granite types: 25 years later. Australian Journal of Earth Sciences, 48(4), 489–499. DOI: https://doi.org/10.1046/j.1440-0952.2001.00882.x https://www.tandfonline.com/doi/full/10.1046/j.1440-0952.2001.00882.x
5. Clemens, J. D. (2003). S-type granitic magmas—Petrogenetic issues, models and evidence. Earth-Science Reviews, 61(1–2), 1–18. DOI: https://doi.org/10.1016/S0012-8252(02)00107-1 https://www.sciencedirect.com/science/article/pii/S0012825202001071
6. Frost, B. R., Barnes, C. G., Collins, W. J., Arculus, R. J., Ellis, D. J., & Frost, C. D. (2001). A geochemical classification for granitic rocks. Journal of Petrology, 42(11), 2033–2048. https://doi.org/10.1093/petrology/42.11.2033
7. Frost, C. D., & Frost, B. R. (2011). On ferroan (A-type) granites: Their compositional variability and modes of origin. Journal of Petrology, 52(1), 39–53. DOI: https://doi.org/10.1093/petrology/egq070 https://academic.oup.com/petrology/article/52/1/39/1468152
8. Hayatu, R. A. (2024). Geochemistry and genetic implications of basement rocks around Makarfi Area, Northwestern Nigeria Basement Complex. FUDMA Journal of Sciences, 8(3), 319–330. DOI: https://doi.org/10.33003/fjs-2024-0803-2552
9. Irzon, R. (2013). Contrasting two facies of Muncung Granite in Lingga Regency using major, trace, and rare earth element geochemistry. Indonesian Journal on Geoscience, 2(1), 23–33. DOI: https://doi.org/10.17014/ijog.2.1.23-33
10. Moyen, J.-F., Laurent, O., Chelle-Michou, C., Couzinié, S., Vanderhaeghe, O., Zeh, A., Villaros, A., & Gardien, V. (2017). The secular evolution of Earth's mantle and crust as recorded by granitic magmatism. Geological Society, London, Special Publications, 449, 357–386. DOI: https://doi.org/10.1144/SP449.8 https://www.lyellcollection.org/doi/10.1144/SP449.8
11. Odewumi, S. C., & Olarewaju, V. O. (2013). Petrogenesis and geotectonic setting of granitic rocks in Idofin–Osi–Eruku Area, Southwestern Nigeria. Journal of Geology & Geosciences, 2(1), 109. https://doi.org/10.4172/2329-6755.1000109
12. Ogah, A. J., & Abubakar, F. (2024). Solid mineral potential evaluation using integrated aeromagnetic and aeroradiometric datasets. Scientific Reports, 14, 1637. https://doi.org/10.1038/s41598-024-52270-6
13. Ojo, O. F., Osazuwa, B. I., Chiemeke, C. C., Osumeje, O. J., Oyedele, A. A., Adagunodo, T. A., Oyeyemi, K. D., & Ejiga, E. G. (2024). Classification of the basement complex using aeromagnetic and remote sensing data analyses: Case study of Ekiti State, southwestern Nigeria. Earth Sciences Malaysia, 8(2), 158–162. https://doi.org/10.26480/esmy.02.2024.158.162

14. Olade, M. A. (2020). Mineral Deposits and Exploration Potential of Nigeria. Amsterdam: Elsevier. https://books.google.com/books?id=vjj1DwAAQBA
15. Oyebamiji, A., Akinola, O., Olaolorun, O., Abdu-Raheem, Y., Adeoye, A., & Oguntuase, M. (2024). Geochemistry, petrogenesis and geological implication of granitic rocks in Igarra Area, Southwestern Nigeria. Energy Exploration & Exploitation, 133(3). DOI: https://doi.org/10.1177/25726838241273519
16. Oyinloye, A. O. (2011). Geology and geotectonic setting of the basement complex rocks in Southwestern Nigeria: Implications on provenance and evolution. DOI: https://doi.org/10.5772/26990
17. Peccerillo, A., & Taylor, S. R. (1976). Geochemistry of Eocene calc-alkaline volcanic rocks from the Kastamonu Area, northern Turkey. Contributions to Mineralogy and Petrology, 58(1), 63–81. DOI: https://doi.org/10.1007/BF00384745
18. Rahaman, M. A. (1988). Recent advances in the study of the Basement Complex of Nigeria. In Precambrian Geology of Nigeria (pp. 11–43). Geological Survey of Nigeria. https://www.sciepub.com/reference/318092
19. Rollinson, H. R. (1993). Using Geochemical Data: Evaluation, Presentation, Interpretation. Harlow, UK: Longman Scientific & Technical. https://books.google.com/books?id=L44sY6RX8_cC
20. Rollinson, H. R., & Pease, V. (2021). Using Geochemical Data: To Understand Geological Processes (2nd ed.). Cambridge: Cambridge University Press. DOI: https://doi.org/10.1017/9781108777834 https://www.cambridge.org/core/books/using-geochemical-data/426537667EEB68205371A28DF9B2FFD5
21. Rose, A. W., Hawkes, H. E., & Webb, J. S. (1979). Geochemistry in Mineral Exploration (2nd ed.). London: Academic Press. https://openlibrary.org/books/OL33090211M
22. Salako, K. A., Adetona, A. A., Rafiu, A. A., Augie, A. I., Jimoh, M. O., Alkali, A., Muriana, R. A., & Lawrence, J. O. (2024). Integrated geophysical investigation for gold mineralization potential over the southern parts of Kebbi State, northwestern Nigeria. Heliyon, 10(14), e34093. https://doi.org/10.1016/j.heliyon.2024.e34093
23. Shand, S. J. (1943). Eruptive Rocks: Their Genesis, Composition, Classification, and Their Relation to Ore-Deposits (2nd rev. ed.). London: Thomas Murby & Co.; New York: John Wiley & Sons. WorldCat (1943 Revised 2nd Edition) Open Library (1943 2nd Revised Edition)
24. Verma, S. P., & Agrawal, S. (2011). New tectonic discrimination diagrams for basic and ultrabasic rocks using high field strength element (HFSE) ratios. Revista Mexicana de Ciencias Geológicas, 28(1), 24–44. https://rmcg.geociencias.unam.mx/index.php/rmcg/article/view/608